ELSEVIER

Coordination Chemistry Reviews
188 (1999) 35–70

COORDINATION CHEMISTRY REVIEWS

www.elsevier.com/locate/ccr

Enlightening organometallic chemistry: the photochemistry of $Fe(CO)_5$ and the reaction chemistry of unsaturated iron carbonyl fragments

Nicholas Leadbeater *

Department of Chemistry, University of Cambridge, Lensfield Road, Cambridge CB2 1EW, UK

Received 12 February 1998; received in revised form 16 September 1998

Contents

* Corresponding author. Tel.: +44-1954-212858; fax: +44-1223-336362.
E-mail address: nel1000@cam.ac.uk (N. Leadbeater)

PII: S0010-8545(98)00217-3

Abstract

Photochemistry offers a simple and often highly selective route to organometallic compounds, overcoming large enthalpy barriers which would otherwise involve elevated temperatures and pressures. Inherent in any photochemical process is the generation of molecules in excited states. In addition, coordinatively unsaturated intermediates are often formed as a result of photolysis of organometallic complexes. A knowledge of the electronic structure, geometry and reaction chemistry of these intermediates is central to the understanding and control of the outcome of the photochemical process. It is the aim of this article to give a general critical discussion of the photochemistry of the mononuclear binary carbonyl $Fe(CO)_5$. Although at first glance this compound seems a simple example, its photochemistry has both fascinated and puzzled chemists for many years and continues to do so today.

Keywords: Photochemistry; Iron carbonyl complexes; Matrix isolation; Ultra-fast spectroscopy

1. Introduction

The photochemistry of organometallic compounds is a new and exciting research area finding applications in synthetic and industrial chemistry. Photochemical processes involve the generation of molecules in excited states and the formation of highly reactive short lived intermediates. It is the aim of this article to give a critical general discussion of the photochemistry of the mononuclear binary metal carbonyl $Fe(CO)_5$, this acting as a prototype for other, more complex, examples. The area has been visited previously, in particular by Poliakoff and Weitz in 1987 [1]. The present article builds on these ideas, reports the results of more recent investigations, and looks at the reactivity of coordinatively unsaturated iron carbonyl fragments with a range of ligands. In the course of this document, square brackets, [ ], will be used to denote coordinatively unsaturated fragments.

On broad-band UV photolysis of $Fe(CO)_5$, dissociation of a carbonyl takes place, this generating the coordinatively unsaturated intermediate $[Fe(CO)_4]$. The quantum yield for CO production in the condensed phase is close to unity [2]. The reaction may proceed further [2,3] and, indeed, photolysis in the gas phase can even yield Fe atoms [2,4–6]. This article will discuss the photochemistry of $Fe(CO)_5$ in low-temperature matrices, in solution and in the gas phase, and will show how this range of complementary experimental techniques have been used to investigate the photochemistry and reaction chemistry of the reactive intermediates formed.

2. Structure and bonding in $M(CO)_5$ [M = Fe, Ru, Os]

The binary carbonyl complexes $M(CO)_5$ (M = Fe, Ru, Os) are trigonal bipyramidal, D_{3h}, in geometry, although there is still contention regarding the relative M–C (equatorial) and M–C (axial) bond lengths [7]. Assuming this D_{3h} geometry, the molecular structure and d-orbital splitting scheme are shown in Fig. 1 [8]. Of lowest energy is the e″ set which, in the absence of ligand orbitals of π symmetry, is entirely metal xz and yz in character. At somewhat higher energy lies the e′ set which are primarily metal xy and x^2-y^2 in character with a small antibonding contribution from equatorial σ orbitals. The most important feature of the e′ orbitals is the observed hybridisation of the metal component away from the equatorial ligands and it is this that governs any subsequent π-interaction [9]. At highest energy lies the z^2 orbital which is of a_1' symmetry. This is strongly metal–axial ligand antibonding and weakly metal–equatorial ligand antibonding.

The first dissociation energies of the saturated metal carbonyls $M(CO)_5$ have been predicted theoretically at the MP2 level [10] and also using molecular orbital calculations based on density functional theory [11]. The ordering of the M–CO bond strengths has been found to be Fe > Os > Ru. This is, at first, surprising since the Os–CO bond would be expected to be weaker than Ru–CO. However, when determining bond dissociation energies contributions from steric factors, σ-donation, π-back-donation and relativistic effects have to be taken into account. Four electron two-orbital interactions, like those between occupied metal d-orbitals and σ-orbitals on CO in metal carbonyls, are destabilising. This destabilisation is due, in part, to an increase in the electronic kinetic energy caused by the node in the out-of-phase combination from the two-orbital interaction. Relativistic effects can, to some extent, mollify this by increasing the so called mass–velocity term of the electronic kinetic energy [12]. The stabilising relativistic effect is larger for carbonyls of 5d elements than that for the 4d period this explaining the ordering of M–CO bond strengths.

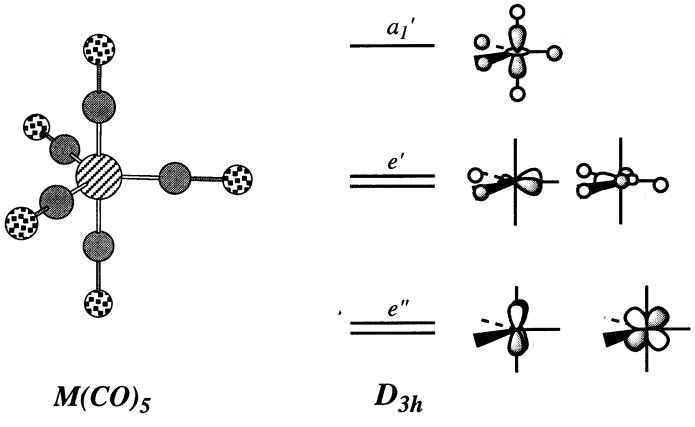

Fig. 1. Structure and d-orbital splitting scheme for $M(CO)_5$ (M = Fe, Ru, Os).

The trend Fe > Os > Ru for M–CO bond dissociation energies has also been shown experimentally. Indeed, the thermal substitution reactions of $Fe(CO)_5$ are so slow and the complex so volatile that a study of the reaction kinetics is difficult [13]. In $Ru(CO)_5$ the carbonyl groups are substitution labile, forming substitution products $Ru(CO)_4L$ readily on addition of a ligand L [14]. As this article will show, photochemistry has allowed for the rationalisation of these observations as well as offering a route to the generation of substituted carbonyl complexes at room temperature and pressure.

3. The photochemistry of $Fe(CO)_5$ in low-temperature matrices

The greatest insight into the structure and properties of coordinatively unsaturated carbonyl fragments has come from matrix-isolation experiments [2,15,16]. This technique involves trapping reactant molecules in an excess of a relatively inert matrix such as a frozen gas (e.g. argon at 20 K) [17]. Reactive fragments are then generated by photolysis. These fragments have long lifetimes since, at such a low temperature, reactions have near zero rate constants. Therefore, once generated, the fragments can be studied spectroscopically in situ by means of conventional IR or UV–vis techniques.

Work by Poliakoff and Turner has shown that broad-band UV photolysis of matrix trapped $Fe(CO)_5$ leads to the generation of $[Fe(CO)_4]$. It was thought initially that $[Fe(CO)_4]$ had a slightly distorted C_{3v} structure [18]. This was later proven to be incorrect on the basis of isotope experiments. Isotopic enrichment offers a unique insight into the molecular structure of matrix-isolated metal carbonyl fragments [19,20]. By means of a force-field approach, the expected positions of the bands in the C–O stretching region of the IR spectrum for a range of proposed geometries can be determined [21–23]. Studies using $^{13}C^{16}O$ have shown that the observed spectrum for $[Fe(CO)_4]$ agrees better with that predicted

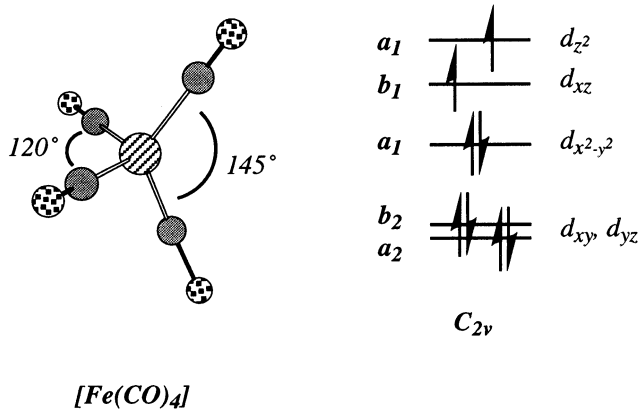

Fig. 2. Proposed structure and d-orbital splitting scheme for C_{2v} $[Fe(CO)_4]$.

for a C_{2v} geometry rather than C_{3v} (Fig. 2) [15]. This is confirmed by $^{12}C^{18}O$ enrichment experiments [24], the resolution of the bands of the different isopotomers being greater than in the case of $^{13}C^{16}O$ due to the greater mass difference in $^{12}C^{18}O$.

Bond angles in $[Fe(CO)_4]$ have been calculated from the relative intensities of the IR bands, this process being simplified because the C–O stretching vibrations in carbonyl complexes can be treated as if they were totally uncoupled from other vibrations within the molecule [16,25]. The calculated bond angles vary slightly from one matrix to another; SF_6 (144, 114°), Ar (147, 120°), CH_4 (150, 120°) [15]. This being said, the values are within experimental error considering the uncertainty caused by the measurement of band intensities, this implying that it is unlikely that the structure is imposed on the molecule by the matrix. The proposed structure of $[Fe(CO)_4]$ in matrices is shown in Fig. 2.

Using a simple molecular orbital method, Burdett has calculated the minimum internal energy (MIE) structures of binary transition metal carbonyls [26]. The observed bond angles of $[Fe(CO)_4]$ are close to those predicted for the MIE C_{2v} geometry of $[M(CO)_4]$ with a triplet ground state. This paramagnetism has been confirmed by magnetic circular dichroism (MCD) studies on matrix isolated $[Fe(CO)_4]$ [27,28]. The MCD spectrum of $Fe(CO)_5$ isolated in an argon matrix does not change over the temperature range 5–25 K. However, UV photolysis of the matrix, generating $[Fe(CO)_4]$, leads to a significant change in the MCD spectrum and also the signal becomes temperature dependent, this being indicative of a paramagnetic species.

In addition to $[Fe(CO)_4]$, in situ generation matrix-isolation studies have allowed for the study of other coordinatively unsaturated iron carbonyl complexes. The tricarbonyl complex $[Fe(CO)_3]$ is generated by photolysis of matrix-isolated $[Fe(CO)_4]$ [29]. Since two IR bands are observed for $[Fe(CO)_3]$, a planar D_{3h} geometry is not plausible. By using isotope labelling, a C_{3v} geometry has been assigned to the fragment (Fig. 3). This is in agreement with calculations by Burdett, using the MIE approach, for a high-spin d^8 $[M(CO)_3]$ complex, again pointing towards a triplet ground state for $[Fe(CO)_3]$. Using the relative intensities of the IR bands in $[Fe(CO)_3]$, the CO–Fe–CO bond angle has been estimated as ca. 108°, this comparing favourably with a calculated value of 111° for the MIE structure.

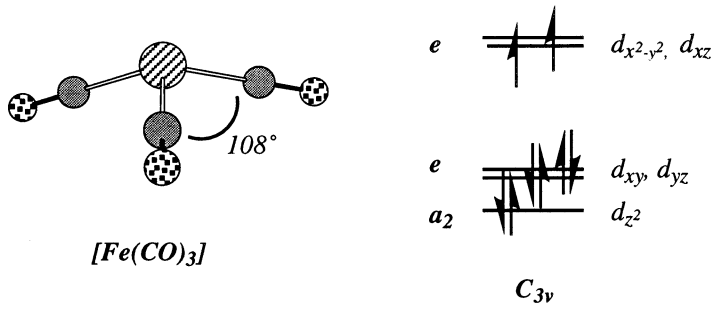

Fig. 3. Proposed structure and d-orbital splitting scheme for C_{3v} $[Fe(CO)_3]$.

Prolonged photolysis in methane and di-nitrogen matrices leads to the formation of further carbonyl species, proposed as $[Fe(CO)_2]$ and [Fe(CO)] [24]. Eventually, iron atoms are formed, indicating that all the carbonyl groups can be removed from $Fe(CO)_5$.

Experiments have also been undertaken using greater concentrations of $Fe(CO)_5$ in the matrix [15]. It is often the case that, in greater concentration, matrix-trapped unsaturated metal carbonyl fragments polymerise as has been illustrated in the case of the photolysis of $Mo(CO)_6$ [30]. Even at concentrations as low as 1 in 1000, measurable concentrations of polynuclear carbonyl complexes are formed on photolysis of $Fe(CO)_5$ in methane matrices (Scheme 1). Spectroscopic data suggest that $[Fe_2(CO)_8]$ and $Fe_3(CO)_{12}$ are the main products generated. The $[Fe_2(CO)_8]$ generated may well be formed from $Fe_2(CO)_9$, the latter being extremely photosensitive in low-temperature matrices losing CO [31]. These results are commensurate with $[Fe(CO)_4]$ being an intermediate in photochemical formation of the polynuclear carbonyl complexes.

The molecular geometry of coordinatively unsaturated binary iron carbonyls has been also been studied in low-temperature matrices generated by co-condensation of iron atoms with noble gas/CO gas mixtures [32]. Co-condensation experiments allow for the direct generation of unsaturated complexes, the product distribution being controlled by the metal concentration. As with the in situ matrix-isolation studies, it is possible to use isotopic labelling as a tool in co-condensation experiments. In a Kr matrix, $[Fe(CO)_2]$ exhibits one band in the CO stretching region of the IR spectrum at 1860 cm^{-1}, this being indicative of a linear $D_{\infty h}$ structure for the fragment, as has been reported for most of the metal di-carbonyls formed in matrices [33]. This value differs from that reported by Poliakoff for $[Fe(CO)_2]$ of 1917 cm^{-1} [29], this peak also being seen in matrix studies on $H_2Fe(CO)_4$ [34]. The co-condensation studies suggest that the 1917 cm^{-1} peak may be an artifact of impurities in the matrix-isolated samples but the exact reason for the discrepancy in reported values for $[Fe(CO)_2]$ is still unknown.

The monocarbonyl [Fe(CO)] shows a ν(CO) absorption at 1884 cm^{-1} in the IR spectrum [32]. This is interesting since it reverses the trend that the more coordinatively unsaturated the iron carbonyl species is, the lower the frequency of the IR absorption. This has also been observed in studies of the photochemistry of $Cr(CO)_6$, $[Cr(CO)_2]$ absorbing at a higher frequency than $[Cr(CO)_3]$ [35]. This effect can be rationalised by consideration of the possible magnitude of the energy-factored force constants and interaction constants for unsaturated metal carbonyls [16,36].

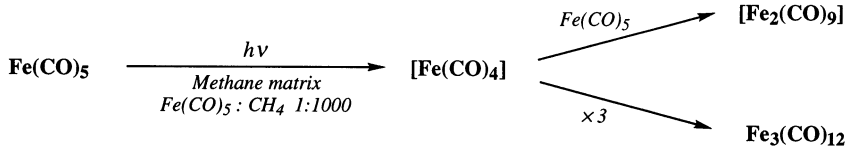

Scheme 1.

In an attempt to understand more fully the structure and bonding in the binary iron carbonyl fragments, Mössbauer studies have been undertaken [37]. Looking specifically at iron carbonyls, there are a number of ways in which bonding can effect Mössbauer isomer shifts. These include π back-bonding from the iron 3d-orbitals to CO resulting in decreased 3d screening of the 4s electrons, σ donation from CO to the iron 3s orbital and the effective radial expansion of the 4s bonding orbitals on Fe on formation of a metal carbonyl complex [38,39]. The first factor decreases the isomer shift, the latter two increase it.

The isomer shift reported for [Fe(CO)] (-0.6 mm s^{-1}) is considerably lower than that calculated for a free iron atom ($+1.0$ mm s^{-1}) [40]. This is indicative of strong π interaction between the iron atom and CO ligand. These values can compared to those reported for [Fe(NH_3)] ($+0.6$ mm s^{-1}) [41] and [Fe(η^2-C_2H_4)] ($+0.55$ mm s^{-1}) [42] where, in the case of ammonia there is no possibility of π interaction with iron and with ethene, although there is the possibility for such an interaction, the effects would be less than for CO [43]. It is also of interest that an iron atom will react with only one ammonia or ethene molecule under co-condensation conditions. Back-donation from the metal atom perhaps makes the iron more susceptible to consecutive reactions with CO by providing a mechanism that depletes its electronic population.

As more CO groups are added to the iron centre, the σ-electron population at the iron nucleus will increase. Consequently, a decrease in isomer shift would be expected. However, shifts of -0.28, -0.18 and $+0.15$ mm s^{-1}) are reported for [$Fe(CO)_2$], [$Fe(CO)_3$] and [$Fe(CO)_4$], respectively. These results have been explained in terms of either increasing σ-donation to the iron 3d orbital or increasing 4s orbital expansion as more CO ligands are attached. Clearly it is difficult to draw definitive conclusions regarding the trends observed beyond the simple MO arguments given here.

4. The photochemistry of $Fe(CO)_5$ in solution

There have been relatively few studies on the transient intermediates formed on photolysis of $Fe(CO)_5$ in solution. In contrast, transient species observed from $Cr(CO)_6$ in solution have been investigated extensively and their structure explained by reference to matrix isolation data [44,45]. For solution studies, in general, the reactive intermediates are produced by irradiation of the starting materials with a short duration pulse from a UV source; this being called flash-photolysis. The concentration of a reactive intermediate is then monitored by means of a second light source producing a longer, less intense, flash of light at a wavelength which is absorbed by the species under investigation. UV–vis flash-photolysis has been useful in many instances but the limitation when applied to organometallic systems is that there is little or no variation between the UV–vis spectra of different intermediates. For this reason, $Fe(CO)_5$ has been studied most productively using IR-monitored flash photolysis, this being termed time-resolved IR (TRIR) spectroscopy. Benzene is a good solvent for solution flash-photolysis experiments

because it can act as a stabilising ligand for any photofragments formed. However, it absorbs strongly in part of the CO spectral range so the hexa-deuterated analogue C_6D_6 is used as this is transparent between 1800 and 2100 cm^{-1} thereby allowing unperturbed TRIR study of the entire spectral range of interest.

On photolysis of $Fe(CO)_5$ in C_6D_6, the C_{2v} iron tetracarbonyl complex $Fe(CO)_4{\cdot}(C_6D_6)$ is formed. Although the nature of bonding of the $[Fe(CO)_4]$ fragment to the solvent moiety is unknown, the IR spectrum of $Fe(CO)_4{\cdot}(C_6D_6)$ bears a strong resemblance to that of $Fe(CO)_4(\eta^2$-alkene) adducts, pointing towards η^2-coordination of the aromatic ring [46]. The solvated complex decays by first order kinetics yielding, in the case of a CO saturated solution, $Fe(CO)_5$ almost exclusively. If excess $Fe(CO)_5$ is added to the solution, $Fe(CO)_4{\cdot}(C_6D_6)$ decays to form what has been proposed as either $[Fe_2(CO)_8]$ or a soluble form of $Fe_2(CO)_9$, these reacting with CO in solution to yield $Fe(CO)_5$. The fact that decay of $Fe(CO)_4{\cdot}(C_6D_6)$ is independent of the concentrations of both CO and $Fe(CO)_5$ suggests that a further intermediate, I, is formed initially. The intermediate may be a spin isomer of $Fe(CO)_4{\cdot}(C_6D_6)$, intersystem crossing being the rate determining step in the decay of $Fe(CO)_4{\cdot}(C_6D_6)$. Other possibilities for I include naked $[Fe(CO)_4]$ or $[Fe(CO)_3]$ or a conformational isomer of $Fe(CO)_4{\cdot}(C_6D_6)$ but these are more difficult to rationalise with the experimental observations. The solution photochemistry of $Fe(CO)_5$ is summarised in Scheme 2.

Photolysis of $Fe(CO)_5$ in cyclohexane at 337 nm in the presence of a number of trialkyl phosphine ligands, PR_3, leads to the generation of both $Fe(CO)_4(PR_3)$ and $Fe(CO)_3(PR_3)_2$, the quantum yield for formation of the latter, Φ_{bis}, being not only high but significantly greater than that for the former, Φ_{mono} [47]. Since $Fe(CO)_3(PR_3)_2$ is in excess of $Fe(CO)_4(PR_3)$ even after 1% conversion of $Fe(CO)_5$, and this absorbs essentially all of the light, $Fe(CO)_3(PR_3)_2$ must be formed as a result of a single-photon process. The product distribution is found to be phosphine concentration independent until the concentration of PR_3 drops to a level where it is in competition with $Fe(CO)_5$ for $[Fe(CO)_4]$ and $[Fe(CO)_3L]$. As a consequence, when the concentration of phosphine is substantially greater than that of $Fe(CO)_5$, formation of $Fe(CO)_3(PR_3)_2$ is favoured over that for $Fe(CO)_4(PR_3)$. When the concentration of phosphine is substantially less than that of $Fe(CO)_5$, formation of the monosubstituted product is favoured.

One explanation for the formation of bis-substituted products as a result of a single-photon process would be the simple stepwise dissociation of two carbonyl

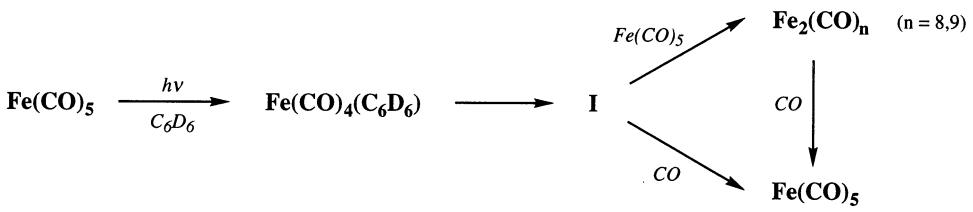

Scheme 2.

groups from $Fe(CO)_5$ to generate $[Fe(CO)_3]$ followed by reaction with two equivalents of ligand. However, after the dissociation of the first carbonyl from $Fe(CO)_5$, the nascent $[Fe(CO)_4]$ will not have enough vibrational energy for further CO dissociation to compete with vibrational relaxation in solution [48,49]. Another possible explanation for the observations is that $[Fe(CO)_3]$ is formed not from a photochemically-excited species but from $[Fe(CO)_4]$ after thermal equilibration with the solvent. Such a mechanism has been proposed for the thermal substitution of triphenylphosphine for alkene in $Fe(CO)_4(\eta^2$-styrene) [50]. The strength of the $[Fe(CO)_3–(CO)]$ bond rules out this possibility since the rate of this reaction would be too slow to be significant on the timescale of the experiments reported. Also, if this mechanism was in action, the product ratio would be dependent on ligand concentration, something that is known not to be the case.

The most feasible mechanism proposed to date centres around the triplet nature of the ground state of $[Fe(CO)_4]$ (Scheme 3). The mechanism does however rely on the assumption that reaction of triplet $[Fe(CO)_4]$ with a ligand, L, occurs before intersystem crossing (ISC) to the singlet potential energy surface. Therefore, attack of L on triplet $[Fe(CO)_4]$ will lead initially to triplet $Fe(CO)_4L$. Although this is a fair assumption, there is no direct evidence for this order for ligand attack and ISC processes. The triplet $Fe(CO)_4L$ proposed can undergo either ISC, producing singlet $Fe(CO)_4L$, or carbonyl dissociation to yield triplet $[Fe(CO)_3L]$, this then reacting with ligand and undergoing ISC to give $Fe(CO)_3L_2$.

Clearly, the product distribution will be controlled by the fate of triplet $Fe(CO)_4L$, ISC leading to the mono-substituted product whilst CO dissociation can lead potentially to the bis-substituted product. The electronic properties of triplet $Fe(CO)_4L$ will be dependent on the nature of L, this effecting both the strength of the Fe–CO bonds in $Fe(CO)_4L$ and the singlet–triplet energy difference.

The 337 nm solution photochemistry of $Fe(CO)_5$ with other two electron ligands has also been investigated with which the results can be compared and contrasted [42]. With pyridine, $Fe(CO)_3(py)_2$ is formed only when a considerable concentration of ligand is present. With *t*-BuNC, only small quantities of $Fe(CO)_3(t\text{-BuNC})_2$ are formed, Φ_{bis}/Φ_{mono} for a single-photon process being < 0.1. In the case of acetonitrile, no bis-substituted product is observed.

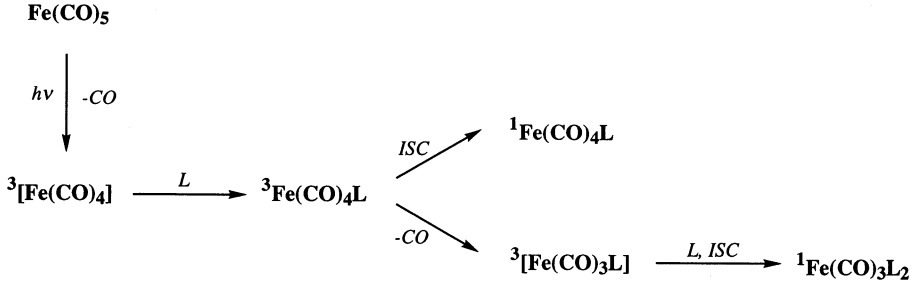

Scheme 3.

On replacing a CO group in $[Fe(CO)_4]$ with a ligand with little π-back bonding capability such as pyridine, the electron density on the metal will be increased. This will increase the relative strengths of the Fe–CO bonds in $[Fe(CO)_4]$ as compared to $[Fe(CO)_3L]$. Although replacement of a CO in $[Fe(CO)_4]$ by a trialkylphosphine to form $[Fe(CO)_3(PR_3)]$ will also lead to an increase in electron density on the metal, the effect will be nowhere near as great as in the case of $[Fe(CO)_3(py)]$. In addition, the singlet–triplet separation in $[Fe(CO)_3(py)]$ may be expected to be smaller than that in $[Fe(CO)_3(PR_3)]$. This is reflected in the experimental results, triplet $[Fe(CO)_3(py)]$ being more likely to undergo ISC than CO dissociation. The opposite is true for triplet $[Fe(CO)_3(PR_3)]$, where CO dissociation is the principal process.

5. The photochemistry of $Fe(CO)_5$ in the gas phase

Considerable attention has been focused on the photodissociation dynamics of $Fe(CO)_5$ in the gas phase. Investigations in the gas phase have the advantage over their solution counterparts that the 'naked' coordinatively unsaturated species can be studied without the influence of solvent [51]. Even relatively inert matrix gases can coordinate to unsaturated complexes, this sometimes effecting a change in structure of the highly reactive species [52]. In addition, putative measurements of association rate constants can be effected by the finite loss of the associated solvent molecules. Gas phase studies allow for real-time kinetic information to be obtained on coordinatively unsaturated compounds and also offer a far richer photochemistry than in solution [53].

Of particular interest is the observation that species with multiple coordinative unsaturation can be produced by an absorption of a single photon. The optical absorption spectrum for $Fe(CO)_5$ is shown in Fig. 4 together with an approximate energy level scheme, Fe–C bond energies being based on an average value of 117 kJ mol^{-1} [54]. At wavelengths where significant absorption occurs, it is clear that excitation of $Fe(CO)_5$ with UV light is capable of removing from three to five carbonyl groups. The actual pattern of fragmentation depends on the nature of the excited states and the dynamics of the resulting dissociation processes [55].

In order to perform gas phase photolysis experiments, particular apparatus is required. Since gas kinetic collisions occur on a microsecond timescale at a density of ca. 10^{15} molecules cm^{-3}, more sensitive and elaborate systems are required. Any transient absorption experiment must include a method for producing the transient intermediates, a source for probing them, and a detector for observing the change in absorption due to them. The coordinatively unsaturated species are formed by UV photolysis, often using an excimer laser. This source can provide more than enough energy at a number of wavelengths in a short pulse. The laser type, pulse length and operating wavelength varies from one experiment to another but pulses of no more than a few mJ cm^{-3} are used to avoid possible multi-photon absorption processes occurring. The typical wavelengths used for photolysis are 351, 248 and 193 nm, these corresponding to the output from XeF, KrF and ArF excimer lasers,

respectively. Since IR spectroscopy is highly structure sensitive, this is the probe of choice for studying the products from gas phase photolysis of metal carbonyls [56].

5.1. Chemical trapping experiments

Chemical trapping experiments constitute the initial work in the area, this involving reaction of the nascent photoproducts with a trapping ligand such as PF_3. Gaseous mixtures of $Fe(CO)_5$ and PF_3 are irradiated with a pulsed laser source and the resulting products, $Fe(CO)_{5-n}(PF_3)_n$ ($n = 0$–3), identified by gas chromatography [57]. Identification of $Fe(CO)(PF_3)_4$ is limited to reasonable extrapolation from the retention times found for other products and from retention times found in the literature [58]. The relative yields for photodissociation using irradiation sources at 352, 248 and 193 nm are shown in Table 1.

From the data obtained, it is clear that absorption of a single photon by $Fe(CO)_5$ in the gas phase leads to multiple loss of CO, the extent of fragmentation increasing with increasing photon energy. There are two plausible mechanisms for fragmentation of $Fe(CO)_5$ to yield multiply unsaturated products, namely a concerted pathway or a series of sequential processes (Scheme 4).

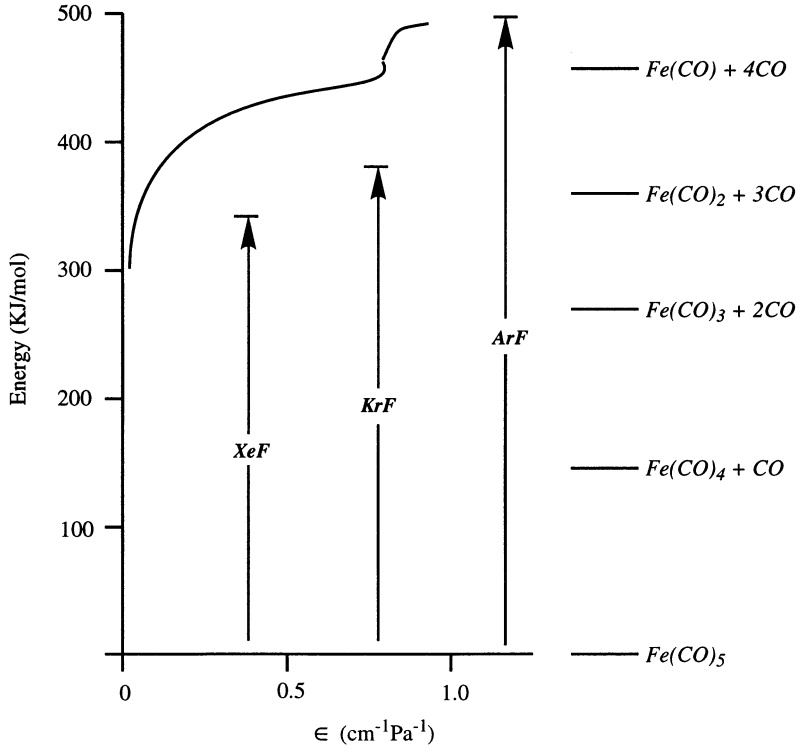

Fig. 4. Absorption spectrum for $Fe(CO)_5$ with an approximate energy level scheme for lasers used in gas-phase photolysis (redrawn from ref. [1]).

Table 1
The excitation conditions and relative yields for the gas phase photodissociation of $Fe(CO)_5$ to give $Fe(CO)_{5-n}$

Photofragment	Relative product distribution (%)											
	Chemical trapping[a]			TRIR[b,c]			Molecular beam (I)[d]			Molecular beam (II)[e]		
	193 nm	248 nm	352 nm	193 nm	248 nm	351 nm	193 nm	248 nm	266 nm	193 nm	248 nm	351 nm
$[Fe(CO)_4]$	9	10	23	0	0	39	0	0	0	0	0	38
$[Fe(CO)_3]$	9	35	46	0	64	61	37	87	98	0	6	62
$[Fe(CO)_2]$	81	55	31	90	36	0	63	13	2	100	94	0
[Fe(CO)]	9	0	0	10	0	0	0	0	0	0	0	0

[a] Taken from Yardley et al., J. Chem. Phys. 74 (1981) 370.
[b] For comparative purposes, the yields of $[Fe(CO)_n]^*$ species are combined with those of the respective $[Fe(CO)_n]$ complexes.
[c] Taken from Weitz et al., J. Phys. Chem. 96 (1992) 2561.
[d] Taken from Waller et al., J. Chem. Phys. 88 (1988) 6658.
[e] Taken from Vernon et al., J. Chem. Phys. 89 (1988) 4092 and 90 (1989) 5510.

Concerted mechanism:

$$Fe(CO)_5^* \longrightarrow [Fe(CO)_4] + CO \quad (4)$$

$$Fe(CO)_5^* \longrightarrow [Fe(CO)_3] + 2CO \quad (5)$$

$$Fe(CO)_5^* \longrightarrow [Fe(CO)_2] + 3CO \quad (6)$$

$$Fe(CO)_5^* \longrightarrow [Fe(CO)] + 4CO \quad (7)$$

Sequential mechanism:

$$Fe(CO)_5^* \longrightarrow [Fe(CO)_4]^\dagger + CO \quad (8)$$

$$[Fe(CO)_4]^\dagger \longrightarrow [Fe(CO)_3]^\dagger + CO \quad (9)$$

$$[Fe(CO)_3]^\dagger \longrightarrow [Fe(CO)_2]^\dagger + CO \quad (10)$$

$$[Fe(CO)_2]^\dagger \longrightarrow [Fe(CO)]^\dagger + CO \quad (11)$$

(*) indicates electronic excitation and (†) internal excitation.

Scheme 4.

The concerted mechanism, although possible, is highly unlikely in the light of the observation that photolysis (350 nm) of $Fe(CO)_5$ in solution and solid matrices yields $[Fe(CO)_4]$ with quantum yields approaching unity. The quenching of any subsequent fragmentation requires the removal of internal energy, a recognised property of the solution phase and matrices. In addition, redistribution of excitation energy often has to occur before dissociation can take place. In as much as this redistribution is statistical, the lowest-energy decay path is favoured over higher-energy ones, this again pointing towards a sequential mechanism.

Excitation of $Fe(CO)_5$ does not place energy directly into a single Fe–C bond [59]. Instead, excitation may result in electronic energy being circulated within the molecule this eventually resulting in the formation of $[Fe(CO)_4]$ and CO. A considerable fraction of the excitation remains within $[Fe(CO)_4]$ as internal vibrational and electronic energy, this then leading to further dissociation. If this is indeed the mechanism in operation, the product distribution from a particular photolysis can be explained in terms of the amount of energy given to the system initially and then the residual internal energy after each subsequent fragmentation [60]. Fragmentation of this sort is well known in mass spectrometry and in radiation chemistry [61,62].

5.2. Further time-resolved IR experiments

TRIR has proven invaluable the study of the photochemistry of $Fe(CO)_5$ in the gas phase [63]. The methods used for gas-phase TRIR experiments are similar to those for solution studies. An inert gas is often added to the photolysis mixture, this both increasing the heat capacity of the system and also dampening the effects resulting from inhomogeneous deposition of photolysis energy or release of energy by relaxation or reaction of nascent photoproducts. In addition, the inert gas acts as a convenient third body in association reactions.

Photolysis of $Fe(CO)_5$ at 193 nm (ArF) leads to a distribution of photoproducts dominated by highly unsaturated species, $[Fe(CO)_2]$ and [Fe(CO)] being formed in an approximate 9:1 ratio. Also, the fragments generated by ArF photolysis display higher levels of internal excitation.

In addition to recombination with CO, both $[Fe(CO)_2]$ and [Fe(CO)] react with parent pentacarbonyl to yield polynuclear products, tentatively assigned as $[Fe_2(CO)_6]$ and $[Fe_2(CO)_7]$, respectively. The $[Fe(CO)_2]$ reacts with parent much more rapidly than [Fe(CO)], the rate constants being 3.7×10^{-10} and 9.2×10^{-11} cm^3 $molecule^{-1}$ s^{-1}, respectively. The $[Fe_2(CO)_7]$ produced reacts further with CO to yield what is thought to be the doubly-bridging isomer of $[Fe_2(CO)_8]$. A remarkable feature in the formation of these polynuclear carbonyls, and those in other studies, is the rate at which they are formed, this often approaching the gas kinetic limit. Such large rate constants would not be expected with the steric requirements involved in the direct collisional formation of these polynuclear products. Instead, it is suggested that an internally excited complex is formed initially, this then facilitating a rearrangement process which, together with energy relaxation, leads to the observed polynuclear products [64].

On 248 nm (KrF) irradiation, $[Fe(CO)_3]$ and $[Fe(CO)_2]$ are formed from $Fe(CO)_5$ in a ratio of ca. 7:3, but no $[Fe(CO)_4]$ is observed. This may be because any $[Fe(CO)_4]$ formed is highly internally excited and readily looses CO to generate the more highly unsaturated intermediates.

After 248 nm photolysis of $Fe(CO)_5$, a further intermediate is formed at a detector limited rate (1 μs), this decaying at the same rate at which $[Fe(CO)_3]$ is formed. This intermediate has been postulated as an excited form of $[Fe(CO)_3]$, $[Fe(CO)_3]$*, which could be in a singlet electronically excited state. On MIE grounds, $[Fe(CO)_3]$* is expected to have a 'T' shaped structure thereby displaying three IR active vibrational modes [65]. One of the vibrations would be expected to be weak and at high frequency. The other modes, A_1 and B_1, would be expected to have a ratio of intensities of 2:1 if all the dipole moment derivatives are equal. Such bands are observed in the TRIR spectrum of KrF laser excited $Fe(CO)_5$. The electronically excited $[Fe(CO)_3]$* is collisionally-quenched very rapidly; this effectively precludes any further study on the intermediate.

The two ground-state photoproducts formed on 248 nm photolysis react both with CO to form mononuclear species and also with $Fe(CO)_5$ to form polynuclear products. The TRIR spectra recorded over the period of 10 μs show the formation of $[Fe_2(CO)_7]$, presumably from the reaction of $[Fe(CO)_2]$ with parent, this then

reacting with nascent CO to yield the doubly bridged isomer of $[Fe_2(CO)_8]$, as in the case of 193 nm photolysis. The product of the reaction of $[Fe(CO)_3]$ with parent has been assigned as the unbridged isomer of $[Fe_2(CO)_8]$ on the basis of comparisons of spectral data with that recorded in low-temperature matrices. In addition, small amounts of $Fe_3(CO)_{12}$ are observed.

On 351 nm photolysis of $Fe(CO)_5$, $[Fe(CO)_4]$ and $[Fe(CO)_3]$ are generated in a ratio of ca. 6:4. Following the expected trend, $[Fe(CO)_4]$ is formed with significant vibrational excitation whilst that of nascent $[Fe(CO)_3]$ is negligible. No $[Fe(CO)_2]$ is detected as opposed to the case of chemical trapping experiments at this wavelength thereby inferring that yields of $[Fe(CO)_2]$ may have been significantly overstated in the chemical trapping work. As in the studies at 248 nm, a novel intermediate is observed on 351 nm photolysis of $Fe(CO)_5$, being postulated as electronically excited $[Fe(CO)_4]^*$, possibly the lowest singlet excited state of $[Fe(CO)_4]$. This assertion is further strengthened by the observation that, in contrast to the ground state triplet $[Fe(CO)_4]$, $[Fe(CO)_4]^*$ reacts rapidly with $Fe(CO)_5$ to yield $Fe_2(CO)_9$. More detailed analysis shows that the IR spectrum of the nascent dinuclear product formed from reaction of $[Fe(CO)_4]^*$ with $Fe(CO)_5$ is not consistent with the lowest energy form of $Fe_2(CO)_9$. Instead, it is proposed that a singly bridged form of the dimer, $[Fe_2(CO)_9]^*$, is formed, this then decaying to the stable, triply-bridged form.

Photogenerated $[Fe(CO)_3]$ reacts with $Fe(CO)_5$ to yield the doubly bridged isomer of $[Fe_2(CO)_8]$ after 351 nm photolysis, just as in the case of the studies at 248 nm. Due to the difference in reactivity between $[Fe(CO)_3]$ and $[Fe(CO)_4]$, $< 1\%$ of the $[Fe(CO)_4]$ reacts with parent by the time all the $[Fe(CO)_3]$ has gone. Indeed, the quantity of $Fe(CO)_5$ consumed by the reaction with $[Fe(CO)_3]$ is measured to be 61% of the quantity of $Fe(CO)_5$ lost due to photolysis, assuming that the initial photoproduct reacts exclusively with this and that the reaction product does not react further with $Fe(CO)_5$.

A further unifying feature between 248 and 351 nm photolyses is the observed formation of $Fe_3(CO)_{12}$. As expected, the formation of the trinuclear carbonyl complex is slower than that of the $[Fe_2(CO)_8]$ isomers which are presumably its precursors. Consistent with this interpretation, the decay of $Fe(CO)_5$ is proportional to the generation of $Fe_3(CO)_{12}$, implying that the rate-determining step in the formation of the trinuclear product is reaction of a coordinatively unsaturated intermediate, possibly an isomer of $[Fe_2(CO)_8]$, with $Fe(CO)_5$. Addition of CO to the photolysis mixture suppresses formation of $Fe_3(CO)_{12}$ thereby indicating that CO also reacts directly with the dinuclear precursor and/or with the coordinatively unsaturated species that lead to the dinuclear precursor.

Interestingly, the polynuclear products formed in the TRIR studies are generated with all the carbonyl groups that were present in the reactants with the exception of $Fe_3(CO)_{12}$ if, as expected, it is formed by reaction of $Fe(CO)_5$ with a coordinatively unsaturated intermediate such as $[Fe_2(CO)_8]$. A potential difference between $Fe_3(CO)_{12}$ and the other polynuclear species discussed here is that, with retention of CO ligands, the other polynuclear complexes are all either electron precise or else coordinatively unsaturated. In the case of the reaction between $Fe(CO)_5$ and $[Fe_2(CO)_8]$, retention of all the carbonyl ligands would result in the formation of a

species that has more than the required number of electrons to satisfy the 18-electron rule

A clear conclusion from the TRIR studies is that the electron spin of the photoproducts governs both their relative distribution and reactivity. An example of this is the reaction of $[Fe(CO)_4]$* with $Fe(CO)_5$ to form an isomer of $Fe_2(CO)_9$ which occurs about 350 times faster than that between ground state $[Fe(CO)_4]$ and parent. As a further test of the influence of spin states of reactants and products on rate constants for photoprocesses, the reaction of $[Fe(CO)_4]$ with O_2 has been studied [59]. Molecular oxygen has a $X^3\Sigma_g^-$, triplet, ground state and, thus, reaction with $[Fe(CO)_4]$ would be expected to occur faster than in the case of a singlet reagent such as CO. This is indeed the case, the reaction of O_2 with $[Fe(CO)_4]$ being in excess of 50 times faster than that of CO.

It is also possible to draw conclusions regarding the spin states of the polynuclear complexes formed in the TRIR experiments. The rapid formation of $Fe_2(CO)_9$ from $[Fe(CO)_4]$* and $Fe(CO)_5$ is compatible with the dimer being formed in a singlet state. Since $[Fe_2(CO)_7]$ is formed rapidly from $[Fe(CO)_2]$ and $Fe(CO)_5$, it is likely that it is formed in a triplet state. The rapid reaction of this dimer with CO to generate the bridged form of $[Fe_2(CO)_8]$ is compatible with this isomer having a triplet ground state. This is confirmed by the observation that it reacts only slowly with CO to yield $Fe_2(CO)_9$. Similarly, since the unbridged isomer of $[Fe_2(CO)_8]$, formed by fast reaction of $[Fe(CO)_3]$ with $Fe(CO)_5$, also reacts slowly with CO, it too is most likely formed in a triplet state. The spin states of [Fe(CO)] and $[Fe_2(CO)_6]$ are not known but, since the former reacts rapidly with parent to form the latter, both these species are probably of the same spin.

As a word of caution, the formally spin-forbidden reaction of $[Fe_2(CO)_8]$ with nascent CO, observed on a millisecond timescale on 351 nm photolysis of $Fe(CO)_5$ occurs to the complete exclusion of trinuclear products despite a 30-fold excess of parent. So, although spin effects are an important predicative factor in determining the magnitude of a rate constant for reaction of coordinatively unsaturated fragments, they are by no means the only determinant. This is reiterated by the observation that the rate of reaction of $[Fe(CO)_3]$ with olefins is an order of magnitude faster than that with CO [66]. Detailed explanations for these discrepancies are still to be found.

TRIR has also been used to study the gas-phase near-IR photolysis of $Fe(CO)_5$, a transversely excited atmospheric (TEA) carbon dioxide laser being used as the irradiation source [67]. Since metal carbonyls absorb only weakly, if at all, in the tunable range of a TEA laser (909–1111 cm^{-1}, 9–11 μm), it is necessary to add an infrared photosensitiser such as SF_6 to the photolysis mixture [68]. On irradiation of a 1:1 mixture of $Fe(CO)_5$ and SF_6, particles of iron are formed and CO evolved, the SF_6 being totally recovered. The proposed mechanism for the photoreaction is shown in Scheme 5.

Of interest is that the iron particles are formed in the face-centred cubic γ-phase, this being formed usually at between 1183 and 1662 K and therefore not normally isolated at room temperature. Since the photolysis mixture is optically dense, the temperature of the molecules in the irradiated volume of the reaction cell will not

be homogeneous. In addition, the energy distribution of the TEA laser beam is also essentially inhomogeneous. Consequently, very high local temperatures can be obtained, this being sufficient to yield γ-iron in the nucleation step rather than α-iron. Since the laser pulse in the experiment lasts only 100 ns, and because the particles are very small, the iron cools very rapidly without a phase change.

5.3. Molecular beam experiments

Molecular beam experiments complement well the other gas-phase photolysis techniques. In a typical molecular beam experiment, an effusive beam of atoms or molecules is produced by pumping them through a narrow slit into an evacuated vessel [69]. In more recent studies, supersonic nozzle sources have been employed, these producing far greater beam intensities as compared to simple effusive techniques [70]. Just as in the case of the chemical trapping and TRIR studies, the photolysis source used in molecular beam experiments is usually an excimer laser; either ArF, KrF or XeF. This is directed orthogonally to the molecular beam and the photodissociation fragments detected using either time-of-flight mass spectroscopy (TOF-MS) or laser induced fluorescence (LIF) techniques [71]. Detection techniques such as vacuum ultraviolet LIF (VUV-LIF) are also valuable for the study of the photodissociation of metal carbonyls because they allow for the direct determination of the rotational, J, and vibrational, v, distribution of the CO photofragments produced. Analysis of the Doppler profile for selected CO lines yields can also provide information about translational energy release.

The small number of molecules in a typical molecular beam may be expected to limit the sensitivity of the experiments. However, the rotational cooling that occurs in a collimated beam results in a collapse of the overall intensity of a band into many fewer rotational transitions, thereby increasing the sensitivity greatly. By fixing the laser wavelength so that it overlies a single vibronic transition, population of a single vibronic level may be achieved. Due to the collision-free conditions in the region of the jet where molecular flow is occurring, fluorescence from molecules in this region will be from the single vibronic level which was populated by absorption of the laser radiation.

$$\mathbf{SF_6 + \mathit{n}\,h\nu \longrightarrow [SF_6]^* \quad (12)}$$

$$\mathbf{[SF_6]^* + Fe(CO)_5 \longrightarrow [Fe(CO)_5]^* + SF_6 \quad (13)}$$

$$\mathbf{[Fe(CO)_5]^* \rightleftharpoons [Fe(CO)_4] + CO \quad (14)}$$

$$\mathbf{[Fe(CO)_{4\text{-}n}] + X^* \longrightarrow [Fe(CO)_{4\text{-}n}]^* + X \quad (15)}$$

$$\mathbf{[Fe(CO)_{4\text{-}n}]^* \rightleftharpoons [Fe(CO)_{3\text{-}n}] + CO \quad (16)}$$

$$\mathbf{Fe \longrightarrow \gamma\text{-iron particles} \quad (17)}$$

Scheme 5.

Molecular beam experiments have the potential to answer questions regarding the collisional stability and reactivity of primary photoproducts. Both the chemical trapping and the TRIR studies of $Fe(CO)_5$ were performed at relatively high pressures where the primary photofragments have undergone many collisions prior to detection. Molecular beam experiments remove these added complications.

Results from molecular beam studies on 193 nm photolysis of $Fe(CO)_5$ serve to confirm that the photofragmentation of $Fe(CO)_5$ in the gas phase is a multi-step process [72,73]. In addition, the product distribution shows strong evidence for complete thermal equilibrium between all degrees of freedom. As in the other gas phase studies, $[Fe(CO)_2]$ is the principal photoproduct at 193 nm. However, yields of $[Fe(CO)_2]$ in excess of 99% in the molecular beam experiments suggest that, in the high collision environment of chemical trapping and TRIR experiments, a significant quantity of this primary photoproduct is collisionally stabilised or else recombines to form more saturated complexes.

The number of steps involved in the mechanism for the formation of $[Fe(CO)_2]$ from $Fe(CO)_5$ has been calculated by computing the temperature of the CO eliminated in each step according to statistical models and then summing calculated rotational and vibrational distributions for each dissociative step and comparing them with the experimentally observed $CO(v, J)$ state distributions. The best agreement was obtained for a sequential mechanism (Scheme 6).

The molecular beam photofragmentation dynamics of $Fe(CO)_5$ at 248, 266 and 351 nm have been studied using VUV-LIF detection [74]. The results show that the sequential CO dissociation mechanism is essentially wavelength independent. The only noticeable systematic deviation between the results obtained from microcanonical statistical calculations and from experimental studies occurs for the CO ($v = 0$) products with low J, where more product is observed than calculated. This deviation represents only a small amount of the total CO product and has been attributed to clustering of $Fe(CO)_5$ molecules this contaminating the beam [75]. Due to the greater concentration of their signal, even a small amount of clustering in the beam will alter the experimental results significantly.

The studies show that product distributions are independent of the delay time between photolysis and probe laser pulses. This both demonstrates the collision free conditions of the molecular beam experiments and also means that the photofragmentation must occur on a timescale faster than that of the experiments, that being 10 ns.

$$\mathbf{Fe(CO)_5} \xrightarrow{h\nu} \mathbf{[Fe(CO)_5]^*} \quad \mathbf{(18)}$$

$$\mathbf{[Fe(CO)_5]^*} \xrightarrow{h\nu} \mathbf{[Fe(CO)_4]^* + CO} \quad \mathbf{(19)}$$

$$\mathbf{[Fe(CO)_4]^*} \xrightarrow{h\nu} \mathbf{[Fe(CO)_3]^* + CO} \quad \mathbf{(20)}$$

$$\mathbf{[Fe(CO)_3]^*} \xrightarrow{h\nu} \mathbf{[Fe(CO)_2]^* + CO} \quad \mathbf{(21)}$$

Scheme 6.

Attempts have been made to investigate further the possibility of there being an excited state, singlet channel for photodissociation of $Fe(CO)_5$ as suggested from the TRIR experiments. The energy difference between the low spin and high spin states of $[Fe(CO)_4]$ and $[Fe(CO)_3]$ is of the order of 1 eV [76]. By assuming that the energy involved in electronic excitation of the unsaturated iron carbonyl fragments is not significant, a complete microcanonical calculation for the excited state channel has been undertaken. Unfortunately, the temperatures of the CO produced when photofragmentation occurs along the excited state manifold fall within the range of that which results from passage along the ground state pathway. As a consequence the existence or absence of the excited state pathway can not be proven definitively. Having said this, by evaluating the χ^2 deviation for various theoretical distributions, the experimental data is well modelled by distributions which are composed with up to 20% of the excited state channel. This is not a definitive test for the excited state manifold but does indicate that the main channel is that passing through the ground states. This is corroborated by the fragment distributions, $[Fe(CO)_2]$ being the main product at 193 nm. If the excited state channel was operative the major product would be $[Fe(CO)_3]$. Whilst excited state processes do not dominate the 193 nm photolysis of $Fe(CO)_5$, irradiation of $Ni(CO)_4$ at this wavelength results almost completely in the production of excited state $[Ni(CO)_n]^*$ products [77].

5.4. Kinetics of the photodissociation of $Fe(CO)_5$

If the photodissociation of $Fe(CO)_5$ into fragments occurs in a sequential manner, the reaction may be described using unimolecular kinetics. The first step of the reaction, namely the absorption of a photon by $Fe(CO)_5$ and the subsequent formation of vibrationally excited $[Fe(CO)_4]^*$, can be interpreted in two ways. Either a rapid randomisation of the photon energy in $Fe(CO)_5$ occurs which then leads directly to dissociation or a fast dissociation takes place with strong coupling between all available product channels, leading to a statistical outcome. The dissociation of excited $[Fe(CO)_4]^*$, and of subsequent excited $[Fe(CO)_n]^*$ fragments, is best modeled by the Rice–Ramsberger–Kassel–Marcus (RRKM) theory. This allows for the determination of the various rate constants from the numbers and frequencies of the vibrational modes and also takes into account the effects of molecular rotation.

Since in the photodissociation of $Fe(CO)_5$ a distribution of photoproduct internal energies can be produced, there will be a range of rate constants, $k(E)$, for the loss of a carbonyl group from an internally excited coordinatively unsaturated fragment. Carbonyl loss can be inhibited by collisional relaxation of the internal energy distribution, hence a pressure dependence of the photoproduct distribution may be expected. For a given photodissociation pathway, when two or more photoproducts are formed, the distribution will be dependent on both the relative values of $k(E)$ and also the rate of collisions at the experimental pressure; some molecules having the energy to dissociate further and some not. It would then be predicted that an increase of pressure in the system would lead to a shift of the product distribution

towards the more saturated photoproducts. This is indeed observed in the case of 248 nm photolysis of $Fe(CO)_5$. However, this is not the case at the other irradiation wavelengths studied. This is in sharp contrast to the case of the Group 6 carbonyls where TRIR experiments have shown that the relative ratios of photoproducts are effected significantly by the pressure of the inert gas at a number of wavelengths [78]. The origin of this difference lies in the fact that, for $Fe(CO)_5$, there are multiple potential energy surfaces for the generation of the photoproducts. The molecules on each surface can result in the generation of products with a range of internal energies. Collisional relaxation can compete with dissociation on each surface thereby resulting in a potentially pressure dependent product distribution. Since the rate of intermolecular energy transfer is significantly less than that for intramolecular redistribution of energy, the greater the energy input into the system, the less effectively collisions can compete with dissociation. This gives an explanation for why 193 nm photolysis of $Fe(CO)_5$ is not pressure dependent in the experimental pressure range reported. In the case of 248 nm photolysis, the pathway leading to production of $[Fe(CO)_2]$ may take place near the energy boundary between the $[Fe(CO)_2]$ and $[Fe(CO)_3]$ species, such that the collisional quenching of the $[Fe(CO)_2–CO]$ dissociation step is highly dependent on the pressure of the inert gas used. In the case of 351 nm photolysis, like that at 193 nm, the energy input takes the photofragments some way from the energy boundary between $[Fe(CO)_n]$ and $[Fe(CO)_{n-1}]$. Again intramolecular energy rearrangement is faster than intermolecular energy dissipation.

5.5. Summary and conclusions

To summarise the results from the gas-phase UV photolysis investigations, the data from the different studies are drawn together in Table 1.

All the results are in agreement that, at this wavelength, the major photoproduct formed on photolysis of $Fe(CO)_5$ is $[Fe(CO)_2]$. However, at 193 nm, only the chemical trapping experiment shows evidence for the formation of $[Fe(CO)_4]$. This may be due to the relatively highly constrained and hence high collision environment of chemical trapping studies as compared to the TRIR and molecular beam experiments. Alternatively, since the photoproduct distributions in the chemical trapping experiments are measured by reaction with PF_3, there is the possibility of $PF_3–CO$ exchange thereby perturbing the nascent $[Fe(CO)_n]$ distribution.

At 248 nm, the TRIR studies and the molecular beam experiments of Waller et al. agree that $[Fe(CO)_3]$ is the major photoproduct (64 and 87%, respectively), but the molecular beam studies of Vernon et al. differ significantly from this, $[Fe(CO)_2]$ being reported as 94% of the product distribution. Even though Vernon et al. performed their experiments at 0.004 atm as opposed to 0.013 atm in the case of Waller et al., and the pressure dependence of 248 nm photolysis would be expected to favour the formation of $[Fe(CO)_2]$ at lower pressures, the discrepancy between the two sets of results is still significant. It should be stated though that Vernon et al. report that it was not possible to use the experimental time-of-flight distributions to determine independently the branching ratios of $[Fe(CO)_3]$ and $[Fe(CO)_2]$.

Consequently, the product distributions were determined on the basis of experimentally optimised iron carbonyl bond dissociation energies, this having implications on the results and inevitably leading to uncertainty in subsequent interpretation of the data.

6. Multiple-photon absorption in $Fe(CO)_5$

Multiple-photon excitation is a non-linear process and is observed only with high intensities of light. It is the advent of lasers that has made multi-photon experiments possible. For the purposes of this article, the essential feature of a multiple-photon process is that the energy of the individual photons can be stored in such a way that several photons can be used cooperatively. As a consequence, excited states not normally accessible can be populated.

In $Fe(CO)_5$, as well as ligand field excitation, there is the possibility of metal-to-ligand charge transfer (MLCT). From the absorption spectrum of $Fe(CO)_5$, a strong MLCT band is found centred at 200 nm. This MLCT state of $Fe(CO)_5$ has been probed by irradiation using a high intensity 400 nm laser source [79]. The experiments have been performed on the femtosecond, fs, timescale. In a typical experiment, an fs laser is used to excite a molecule to a dissociative state [80]. The products are then detected by time-of-flight mass spectroscopy (TOF ms) with fs resolution [81]. Studying photoprocesses with fs techniques allows for the investigation of ultra-fast processes and can and often does reveal a great deal about the nature of the transition states of the reaction.

The available energy for dissociation of $Fe(CO)_5$ after absorption of two photons of 400 nm is great enough to break all five Fe–CO bonds. The fs experiments show that, after absorption of the two photons, $Fe(CO)_5$ dissociates up to Fe(CO) on a very short timescale of about 100 fs, all the fragments $[Fe(CO)_n]$ ($n = 2$–4) being detected in the TOF mass spectrum. The Fe(CO) fragment further dissociates and looses the remaining carbonyl ligand on a longer timescale of 230 fs. These results, at first glance, point towards a stepwise mechanism for the dissociation. However, the fact that practically the same decay time is recorded for the parent and the $[Fe(CO)_n]$ ($n = 2$–4) fragments suggests that the same intermediate state dynamics determine these transients and hence a concerted mechanism is most likely. In other words, the measured transients for $[Fe(CO)_n]$ ($n = 2$–4) represent snapshots of the evolution of the multi-dimensional transition state of $Fe(CO)_5$, $[Fe(CO)_5]‡$, leading towards the loss of four carbonyl ligands yielding [Fe(CO)]. Study of the decay profile of [Fe(CO)] and the rise time of atomic iron and CO has lead to the conclusion that at least two forms of the [Fe(CO)] fragment are formed in the dissociation and only a small proportion of these undergo the further fragmentation.

As in the case of the ligand field studies, upon two photon excitation of $Fe(CO)_5$, the MLCT excited state formed would initially be in the singlet manifold. Since the resultant photodissociation occurs within a few hundred fs, this being significantly shorter than the time required for a non-adiabatic crossing to a triplet state, it is

most likely that the dissociation proceeds directly from the singlet state of the starting material to some electronically excited singlet state of the fragments.

The idea of a concerted mechanism dominating the photodissociation of metal carbonyls following multi-photon excitation has been discussed previously for the fs photochemistry of $Cr(CO)_6$ [82]. In this case, the parent molecule absorbs two, three or more photons coherently with the formation of a highly excited electronic state. The molecule then dissociates explosively, loosing several ligands simultaneously in the timescale of a single vibration.

7. The reaction chemistry of unsaturated fragments

7.1. Reaction chemistry in matrices

Reactions of matrix isolated $[Fe(CO)_4]$ can be promoted by near-IR irradiation at frequencies of ca. 9000–13000 cm^{-1} [15]. The majority of selective IR induced reactions reported in the literature occur in the gas phase. They involve individual molecules overcoming a high activation energy barrier by rapidly absorbing many low-energy photons, usually from a high-intensity CO_2 laser source. For example, the IR photodissociation of SF_6 requires absorption of ca. 40 photons at ~ 948 cm^{-1} [83]. In low-temperature matrices, the energy barriers for reactions are often relatively small and can be overcome by a molecule absorbing only one IR photon. Due to the low quantum yield of reaction, $[Fe(CO)_4]$ is only affected marginally by the IR irradiation. The energy-transfer process is not fully understood but is believed that the role of the irradiation source is merely to supply thermal energy to the molecules [84,85]. It is not clear if the process involves heating of the matrix in the immediate proximity of the excited molecule but, whatever the situation, the effect is highly localised. Just like UV photolysis, IR-laser-induced processes are highly selective and only the molecules that absorb radiation at the precise wavelength of the IR laser undergo reaction.

IR irradiation of $[Fe(CO)_4]$ in di-nitrogen, methane and some noble gas matrices leads to interaction with the matrix medium [15]. This is reversed and $[Fe(CO)_4]$ regenerated by irradiation with light of $\lambda > 375$ nm. Reaction with di-nitrogen results in the formation of the N_2 substituted complex $Fe(CO)_4(N_2)$ [86]. The formation of di-nitrogen complexes is well reported for a number of transition metal carbonyls in N_2 matrices [87]. By analogy with this, the N_2 group is almost certainly bound end-on (η^1) rather than sideways (η^2). Although original experiments suggested a C_{3v} structure for $Fe(CO)_4(N_2)$, on the basis of both MO calculations and ligand-effect analysis of the IR spectrum, a C_{2v} structure is now considered more likely.

In noble gas matrices, upon IR irradiation of $[Fe(CO)_4]$ there is the potential for formation of substitution products. In xenon, there is definite IR evidence for the formation of $Fe(CO)_4(Xe)$. This is not totally unexpected since it is isoelectronic with the well established stable anion $[Fe(CO)_4I]^-$ [88]. In the case of krypton, results are hard to interpret but the possibility for the formation of $Fe(CO)_4(Kr)$

can not be excluded. There is no observable adduct formation observed in argon matrices.

In the case of methane, $Fe(CO)_4(CH_4)$ is formed, the CH_4 group occupying an equatorial position. It is unlikely that C–H bond cleavage occurs to yield $[HFe(CO)_4]$ or $[CH_3Fe(CO)_4]$ because such ligands would be expected to produce a larger shift in C–O stretching frequency from $[Fe(CO)_4]$ than is observed in the IR spectrum of $Fe(CO)_4(CH_4)$. Since a large excess of methane is required in the matrix to ensure that at least one CH_4 molecule is close to each $[Fe(CO)_4]$ fragment, absorptions due to free methane dominate the C–H stretching region of the IR spectrum and bands attributable to coordinated methane can not be seen. The equatorial position of the methane group is of particular interest since both MO calculations and experimental studies suggest that, for poor π-acceptor ligands such as CH_4, NH_3 and MeCN, an axial site should be favoured [89–91]. The most plausible modes of bonding methane to iron are either a linear M–H–C bond similar to that found in the room temperature crystal structures of a number of molybdenum complexes or a double H bridge analogous to that in BH_4^- in $[Mo(CO)_4(BH_4)]^-$ [92,93].

Of note is that $[Fe(CO)_4]$ can exist in both complexed and uncomplexed forms in methane matrices whereas, in the case of chromium it is not possible to obtain uncoordinated $[Cr(CO)_5]$ under these conditions [94]. This may be as a consequence of the difference in UV absorption spectra of the products or, more simply, as a result of a genuine difference in reactivity; $[Fe(CO)_4]$ having a triplet ground state and $[Cr(CO)_5]$ a singlet [95,96]. This is interesting since, in hydrocarbon solution, $[Fe(CO)_4]$ is considerably more reactive towards added ligands than $[Cr(CO)_5]$, this being the opposite to the case in methane matrices [97]. These results can be understood from the viewpoint that $[Cr(CO)_5]$ is more reactive towards hydrocarbon solvents than $[Fe(CO)_4]$. Consequently, solutions would contain totally complexed $[Cr(CO)_5]$ and only partially complexed $[Fe(CO)_4]$ thereby making $[Fe(CO)_4]$ comparatively more reactive towards added ligands.

The reactivity of $[Fe(CO)_4]$ towards hydrocarbons has been further investigated by UV photolysis of $Fe(CO)_5$ in frozen hydrocarbon glasses (1:4, isopentane:methylcyclohexane) at 77 K [15]. Since the glass is, like methane, a hydrocarbon, similar complexes would be expected. Indeed, photolysis leads to the formation of $Fe(CO)_4$(glass). Prolonged irradiation leads to the generation of an $[Fe(CO)_3]$ type species in the glass, this being reversed by IR irradiation.

All these matrix-isolation experiments show that there is a significant reaction between $[Fe(CO)_4]$ and the matrix material, be it a noble gas or a hydrocarbon. For this reason, and for the others cited previously, care must be taken when interpreting and discussing results from matrix-isolation studies. This being said, since most solution photochemistry is undertaken in hydrocarbon solution, it may be argued that, by studying the interactions of the unsaturated iron carbonyl fragments in hydrocarbon glasses and methane matrices, the solution chemistry of $Fe(CO)_5$ may be better understood.

7.2. Laser-induced intramolecular exchange processes in matrix-isolated [Fe(CO)$_4$]

The IR-photochemistry of [Fe(CO)$_4$] is also interesting due to the intramolecular ligand exchange processes observed when the molecule is irradiated at frequencies of around 2000 cm^{-1} (corresponding to ν_{CO}) [19]. Dynamic intramolecular ligand exchange processes can not be studied at room temperature by conventional IR spectroscopy because the IR timescale is significantly faster than any exchange process. However, in low temperature matrices, once a molecule has been isomerised by laser irradiation, it remains fixed in its new configuration indefinitely. Under these conditions, the isotopic labelling of some of the CO groups in [Fe(CO)$_4$] with $^{13}C^{18}O$ allows for the stereochemistry of rearrangement processes to be investigated by analysis of changes in the C–O stretching region of the IR spectrum. For a C_{2v} four coordinate fragment there is the possibility of both Berry and non-Berry pseudorotation mechanisms. It is only the interconversion of the isomers of [Fe($^{12}C^{16}O$)$_2$($^{13}C^{18}O$)$_2$] which show any spectroscopic differences between the possible intramolecular rearrangement modes. This is because there are three disubstituted isomers and a particular isomer can undergo two possible isomerisations while the mono- and tris-substituted species have only two isomers and one possible isomerisation. The observed laser induced isomerisations of [Fe($^{12}C^{16}O$)$_{4-n}$($^{13}C^{18}O$)$_n$] ($n = 1$–3) are shown in Fig. 5. The principal differences between the two mechanisms are that, in the non-Berry pseudorotation path, the di-axial (AA) isomer can not convert into the di-equatorial (EE) isomer directly. In the Berry psudorotation mechanism, the axial–equatorial (AE) isomer can convert only into itself and not into AA or EE.

The observed isomerisation of [Fe(CO)$_4$] has been rationalised by the use of a topological model, the distortion octahedron [98]. Topological models have been used with considerable success in a number of cases to enumerate isomers and deduce their interconversion pathways [99]. This model is, in reality, a qualitative expression of the Jahn-Teller theorem and the results have been supported by more rigorous analysis [100]. The octahedron allows for the distortions of a tetrahedral four coordinate fragment to the lower symmetry C_{2v} geometry to be mapped. The centre of the octahedron represents the undistorted tetrahedral structure and the vertices represent the C_{2v} geometry. Thus, points along a line joining the centre to a vertex correspond to increasingly distorted (C_{2v}) structures. Similarly, all other points on the surface represent particular distortions from T_d of the fragment and hence any line along or within the octahedron represents a series of geometries along a possible distortion pathway. In the case of [Fe(CO)$_4$] the important parts of the distortion octahedron are the vertices (corresponding to C_{2v} geometry), the centres of the edges (corresponding to C_s geometry) and limits of the C_{2v} distortion coordinate (corresponding to C_{4v} geometry). The distortion octahedron model, with the points of interest delineated, is shown in Fig. 6.

As discussed earlier sections, MIE calculation show that, for [Fe(CO)$_4$] in a triplet ground state, a C_{2v} geometry is most stable. As a result, the centre of the distortion octahedron, T_d, will be an energy maximum and the vertices, C_{2v}, energy minima. Any C_{4v} geometry will be of higher energy than the T_d structure because

the HOMO of C_{4v} [Fe(CO)$_4$] is Fe–C antibonding. Any ground state intramolecular rearrangement will be represented on the distortion octahedron by the lowest energy path connecting two C_{2v} geometries at apices of the octahedron. As both the T_d and C_{4v} structures are energy maxima, there is no direct isomerisation pathway between the apices of the octahedron. Since the equatorial vertices represent energy minima, the lowest energy path for the isomerisation must pass through these points.

By placing the possible isomers of [Fe(^{12}C^{16}O)$_2$(^{13}C^{18}O)$_2$] on the distortion octahedron, the origin of the non-Berry process has been understood [98]. The diaxial isopotomer, AA, is at the top of the octahedron and the diequatorial isopotomer, EE, at the bottom. The vertices around the equator represent enantiomers of the AE isopotomer. There are low-energy paths for AA × AE and for EE × AE but not for AA × EE, thereby explaining the reason for the non-Berry process.

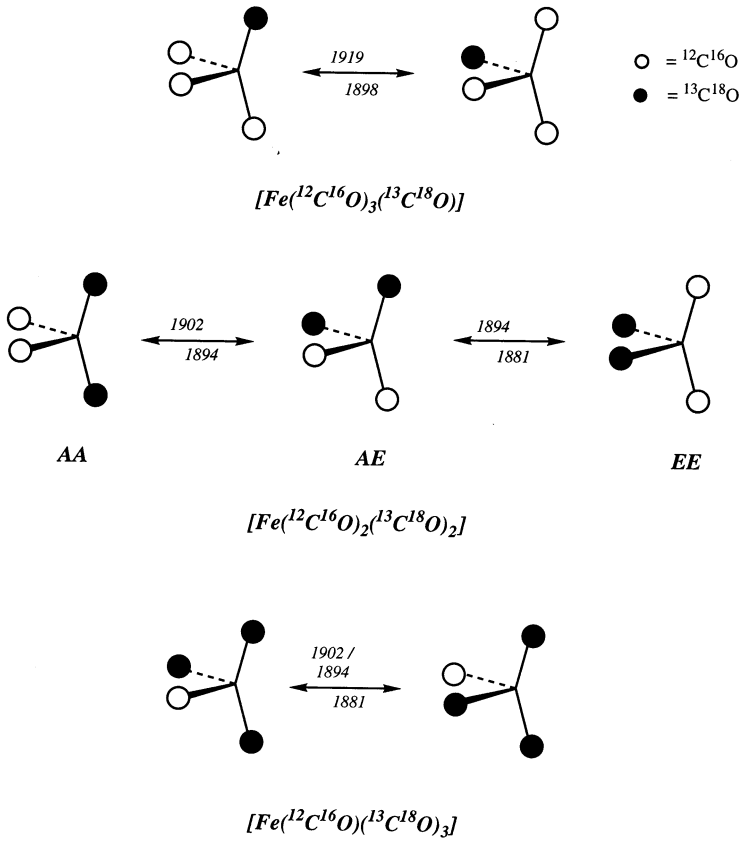

Fig. 5. Observed laser-induced isomerisations of [Fe(^{12}C^{16}O)$_{4-n}$(^{13}C^{18}O)$_n$] (redrawn from ref. [16]). Frequencies reported for isomerisations are in wavenumbers (cm^{-1}).

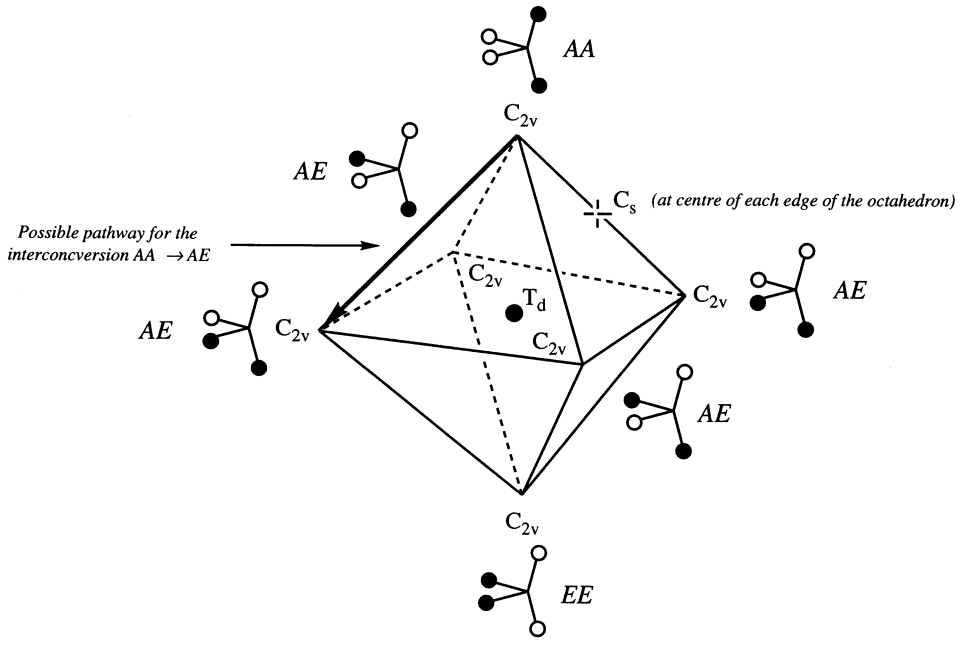

Fig. 6. Distortion octahedron model for $[Fe(CO)_4]$ with the points of interest delineated (redrawn from ref. [98]).

The distortion octahedron provides the first simple rationalisation of the intramolecular rearrangements observed in $[Fe(CO)_4]$. It is, however, reliant on the fact that the lowest energy isomerisation processes are topologically equivalent to the edges of the octahedron, only adjacent vertices being connected by low-energy pathways. The model does not however explain how vibrational energy is transferred from the primarily C–O stretching mode excited by IR irradiation to the C–Fe–C bending modes which cause the isomerisation.

7.3. The gas-phase reaction chemistry of unsaturated intermediates

The gas-phase reactions of $[Fe(CO)_3]$ and $[Fe(CO)_4]$ with a number of substrates have been studied using TRIR spectroscopy. As examples of these investigations, the reaction chemistry of the intermediates with dienes, di-hydrogen, di-nitrogen and with triethylamine will be discussed.

7.3.1. Reaction with dienes

Using molecular orbital theory, $[Fe(CO)_3]$ would be expected to bond more readily with conjugated dienes than with unconjugated ones [101]. In support of this assertion, there are a large number of iron tricarbonyl complexes containing conjugated dienes and there are reports of non-conjugated dienes isomerising to a conjugated species in order to form a stable $Fe(CO)_3$(diene) complex [102]. This

being said, there are also reports both of complexes containing non-conjugated dienes and of stable bis-alkene complexes [103,104]. By studying the interactions of both conjugated and non-conjugated dienes with $[Fe(CO)_3]$ and $[Fe(CO)_4]$ using TRIR, it has been possible to gain a greater insight into the bonding of olefins with metal carbonyl fragments and has also allowed for a more in-depth discussion of the properties of coordinatively unsaturated iron carbonyl fragments [105]. TRIR has also been highly successful in the study of the gas-phase reactions of dienes with $[Cr(CO)_4]$ where it has been shown that the mechanism for reaction of the metal carbonyl fragment with both 1,3-pentadiene (1,3-PD) and 1,4-pentadiene (1,4-PD) is similar, the differences observed being traced principally to the geometry of the substituted products [66]. Interestingly, in the case of $[Cr(CO)_4]$ coordination with non-conjugated dienes is preferred over conjugated dienes.

Reaction of $[Fe(CO)_4]$ with both 1,3- and 1,4-PD is slower than expected, this being attributed to the triplet spin of $[Fe(CO)_4]$ and indicating that the product, $Fe(CO)_4(\eta^2$-PD), has a singlet ground state. This is confirmed by the reported activation energy of the reaction which is small (~ 5.4 kJ mol^{-1}) and the pre-exponential factor which is nearly two orders of magnitude lower than the gas-kinetic limit. Of interest is that the rate of reaction of $[Fe(CO)_4]$ with 1,3-PD is significantly greater than that in the case of 1,4-PD. This difference can be rationalised in terms of entropic effects. Free rotation would not be expected in 1,3-PD or in any complexes formed with it. On the other hand, 1,4-PD shows significant rotation at room temperature and this would be restricted by complexation. Consequently, the reaction of 1,4-PD would have an entropy of activation to complexation that is significantly more negative than that for 1,3-PD, this going some way to explaining the difference in reaction rate with $[Fe(CO)_4]$.

As may be expected, $[Fe(CO)_3]$ reacts much faster than $[Fe(CO)_4]$ with both 1,3- and 1,4-PD, this reflecting the spin allowed nature of interaction with $[Fe(CO)_3]$. Two products are detected in the reaction of $[Fe(CO)_3]$ with 1,3-PD, namely $Fe(CO)_3(\eta^4$-1,3-PD) and $[Fe(CO)_3(\eta^2$-1,3-PD)]. In the case of 1,4-PD, along with $Fe(CO)_3(\eta^4$-1,4-PD) and $[Fe(CO)_3(\eta^2$-1,4-PD)], the agostically-bonded species $[Fe(CO)_3(\eta^{2:CH}$-1,4-PD)] is also formed, where $\eta^{2:CH}$ represents an agostic C–H–Fe interaction.

TRIR spectroscopic data points towards the initial formation of a transient intermediate, $[Fe(CO)_3(PD)]\dagger$ on reaction of $[Fe(CO)_3]$ with PD. The kinetic results suggest that two or more channels are open for reaction of $[Fe(CO)_3(PD)]\dagger$, the processes being competitive. The rate of formation of $Fe(CO)_3(\eta^4$-PD) is dependent on both the buffer gas and PD pressures. This suggests that the initial reaction of $[Fe(CO)_3]$ with PD involves a reversible step. If this was not the case, the reaction would be an elementary bimolecular process occurring under pseudo first-order kinetics and therefore would be dependent only on the pressure of PD. Therefore, $[Fe(CO)_3(PD)]\dagger$ must undergo collisional deactivation to avoid decomposing back to reactants. By using the data from these and other analogous reactions, rate constants for the addition reaction of $[Fe(CO)_3]$ with PD, and for the collisional deactivation and decomposition of $[Fe(CO)_3(PD)]\dagger$ have been estimated. However, no single set of rate constants can account for the experimentally observed data,

indicating that it is not $[Fe(CO)_3(PD)]\dagger$ that is observed but a second intermediate $[Fe(CO)_3(PD)]^*$ for which $[Fe(CO)_3(PD)]\dagger$ is a precursor. The reaction can then be broken into a number of elementary steps, as can be seen in Scheme 7.

Since the reaction of $[Fe(CO)_3]$ and PD is very rapid, the process may well be spin allowed, $[Fe(CO)_3(PD)]\dagger$ most likely being a triplet species. Since the 18-electron $Fe(CO)_3(\eta^4\text{-PD})$ has a singlet ground term, it may also be postulated that $[Fe(CO)_3(PD)]^*$ is a singlet species. Consequently, the formation of $Fe(CO)_3(\eta^4\text{-PD})$ may be expressed as a reaction of $[Fe(CO)_3]$ with PD to form an electronically excited triplet species $[Fe(CO)_3(PD)]\dagger$, this then forming vibrationally and rotationally excited singlet $[Fe(CO)_3(PD)]^*$ by way of a collisionally enhanced crossover between the triplet and singlet potential energy surfaces. This curve crossing must occur since singlet $[Fe(CO)_3]$ is higher in energy than triplet $[Fe(CO)_3]$ but singlet $Fe(CO)_3(\eta^4\text{-PD})$ is lower in energy than triplet $Fe(CO)_3(\eta^4\text{-PD})$.

The formation of $[Fe(CO)_3(\eta^2\text{-PD})]$ from $[Fe(CO)_3(PD)]\dagger$ is temperature dependent, an increase in temperature enhancing the rate of reaction. This behaviour is compatible with a situation in which surmounting an energy barrier is rate limiting in the formation of $[Fe(CO)_3(\eta^2\text{-PD})]$. The rate of formation of $[Fe(CO)_3(\eta^2\text{-PD})]$ is very fast, implying that it is a triplet species. The exact mechanism for the reaction is still in debate but is dependent on the nature of the bonding of the PD to the '$Fe(CO)_3$' moiety in $[Fe(CO)_3(PD)]\dagger$. For example, if the PD group in $[Fe(CO)_3(PD)]\dagger$ is bound in an η^4 mode, the conversion of this intermediate to $[Fe(CO)_3(\eta^2\text{-PD})]$ would involve the cleavage of a metal–ligand bond, this being an activated process in agreement with the observed results. This being said, no conclusions can be drawn since $[Fe(CO)_3(PD)]\dagger$ is inferred but not observed.

The third product, formed on reaction of $[Fe(CO)_3]$ with 1,4-PD, $[Fe(CO)_3(\eta^{2:CH}\text{-1,4-PD})]$, contains an agostic C–H–Fe interaction where one of the open sites on the metal centre is bonded to a methylene hydrogen on the 1,4-PD ligand. Complexes containing these types of agostic interactions are also reported as intermediates in alkyl–alkene isomerisations and diene isomerisations involving coordinatively unsaturated organometallics [106,107]. Since analogous methylene hydrogens are not present in 1,3-PD, this explains why the formation of the agostic product in is unique to 1,4-PD.

$$Fe(CO)_3 + PD \rightleftharpoons [Fe(CO)_3PD]^\dagger \quad (22)$$

$$[Fe(CO)_3PD]^\dagger + X \longrightarrow [Fe(CO)_3PD]^* + X \quad (23)$$

$$[Fe(CO)_3PD]^* + X \longrightarrow Fe(CO)_3(\eta^4\text{-PD}) + X \quad (24)$$

X = collisional partner

Scheme 7.

The TRIR data suggest that, as with the other products, [Fe(CO)$_3$($\eta^{2:CH}$-1,4-PD)] is formed from [Fe(CO)$_3$(PD)]†. The observation that the amount of [Fe(CO)$_3$($\eta^{2:CH}$-1,4-PD)] formed relative to [Fe(CO)$_3$(η^2-1,4-PD)] increases with increasing temperature, infers that the initial activation energy for the formation of [Fe(CO)$_3$(η^2-1,4-PD)] from [Fe(CO)$_3$(PD)]† is greater than that for [Fe(CO)$_3$($\eta^{2:CH}$-1,4-PD)]. The [Fe(CO)$_3$($\eta^{2:CH}$-1,4-PD)] formed is most likely a triplet since it is both generated rapidly from [Fe(CO)$_3$(PD)]† and goes on to form triplet [Fe(CO)$_3$(η^2-1,4-PD)] rather than singlet [Fe(CO)$_3$(η^4-1,4-PD)].

The reaction chemistry of [Fe(CO)$_3$] and [Fe(CO)$_4$] with 1,3- and 1,4-PD is summarised in Scheme 8.

In conclusion, the similarity between the reaction chemistry of [Fe(CO)$_3$] and [Fe(CO)$_4$] with 1,3- and 1,4-PD implies that, as in the case of [Cr(CO)$_4$], the differences in conjugation of the two dienes do not effect the formation of products. However, the reactions of [Fe(CO)$_3$] and [Cr(CO)$_4$] with dienes follow different mechanisms. Whereas all the reactions of [Cr(CO)$_4$] take place on one, singlet, potential energy surface, in the case of [Fe(CO)$_3$] both singlet and triplet potential energy surfaces are involved.

7.3.2. Reaction with di-hydrogen

Reaction of [Fe(CO)$_4$] with dihydrogen leads to the di-hydride complex H$_2$Fe(CO)$_4$ [108]. The rate constant for the reaction is several orders of magnitude slower than for addition of di-hydrogen to other coordinatively unsaturated species because of the triplet nature of [Fe(CO)$_4$] and the proposed singlet ground state of H$_2$Fe(CO)$_4$ [109,110]. In addition, the rate of reaction is, within experimental error, independent of temperature implying that the activation barrier, if any, to the oxidative addition is very small. This implies that the energy necessary to break the H–H bond in H$_2$ must come from the formation of Fe–H bonds. Consequently, initiation of the formation of the Fe–H bonds must come before breakage of the H–H bond implying that the reaction involves a di-hydrogen M–(η^2-H$_2$), intermediate. This is not totally unexpected as di-hydrogen species have often been found to be in equilibrium with di-hydride species [111]. If this is the case here, the equilibrium must lie on the side of the di-hydride as no di-hydrogen complex is detected in the TRIR experiments. Of interest is that with [Fe(CO)(NO)$_2$], there is clear evidence for the formation of the dihydrogen complex Fe(CO)(NO)$_2$(η^2-H$_2$) [112]. This difference in the bonding of H$_2$ can be explained by the fact that, using the Dewar-Chatt (η^2) bonding model, the more π-acidic the metal centre is, the more likely it is that di-hydrogen complexes can be formed rather than di-hydride analogues. The NO ligands in [Fe(CO)(NO)$_2$] reduce the π-donor properties of the metal centre as compared to [Fe(CO)$_4$] with the consequence that cleavage of the H–H bond is prevented.

Reaction of [Fe(CO)$_3$] with H$_2$ yields the di-hydride intermediate [H$_2$Fe(CO)$_3$], the rate of reaction being similar to that for addition of CO to the tricarbonyl to yield [Fe(CO)$_4$] [113]. The reaction occurs considerably more rapidly than in the case of [Fe(CO)$_4$], this reflecting the spin-allowed nature of the process. Since there is no reason to expect that substitution of an H$_2$ for a CO would alter significantly

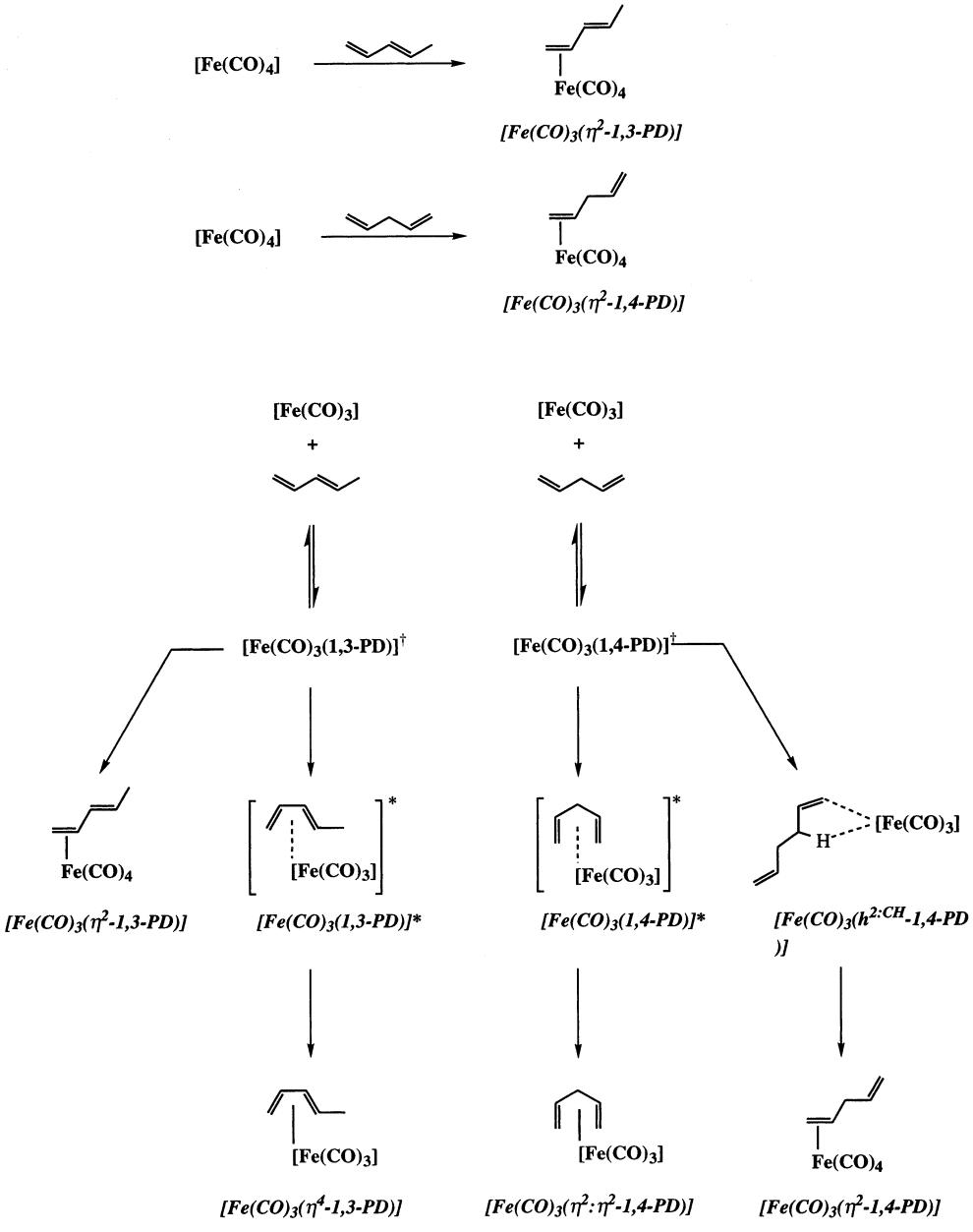
[Fe(CO)4]
Fe(CO)4
[Fe(CO)3(η2-1,3-PD)]
[Fe(CO)4]
Fe(CO)4
[Fe(CO)3(η2-1,4-PD)]
[Fe(CO)3]
+
[Fe(CO)3]
+
[Fe(CO)3(1,3-PD)]†
[Fe(CO)3(1,4-PD)]†
Fe(CO)4
[Fe(CO)3(η2-1,3-PD)]
[Fe(CO)3]
*
[Fe(CO)3(1,3-PD)]*
[Fe(CO)3]
*
[Fe(CO)3(1,4-PD)]*
H
[Fe(CO)3]
[Fe(CO)3(h2:CH-1,4-PD)]
[Fe(CO)3]
[Fe(CO)3(η4-1,3-PD)]
[Fe(CO)3]
[Fe(CO)3(η2:η2-1,4-PD)]
Fe(CO)4
[Fe(CO)3(η2-1,4-PD)]

Scheme 8.

the ligand field energy it is most probable that, like $[Fe(CO)_4]$, $[H_2Fe(CO)_3]$ has a triplet ground state. This is confirmed by its chemistry, ligands such as ethene reacting with $[H_2Fe(CO)_3]$ much more slowly than with $[Fe(CO)_3]$.

7.3.3. Reaction with di-nitrogen and triethylamine

In their reactivity with di-nitrogen and triethylamine, $[Fe(CO)_3]$ and $[Fe(CO)_4]$ form the expected products [114]. With $[Fe(CO)_4]$, $Fe(CO)_4N_2$ and $Fe(CO)_4(NEt)_3$ are formed on reaction with N_2 and NEt_3, respectively. For $[Fe(CO)_3]$, $[Fe(CO)_3N_2]$ and $[Fe(CO)_3(NEt_3)]$ are produced. Again, the reactions with $[Fe(CO)_3]$ occur much more rapidly than with $[Fe(CO)_4]$ for the reasons of spin multiplicity of the metal carbonyl fragments.

8. Summary and outlook

This article has shown that by using a number of different but complementary experimental techniques, it is possible to study the photochemistry of $Fe(CO)_5$ in some detail. Matrix isolation experiments allow for the stabilisation of key unsaturated intermediates and for their geometry and electronic structure to be elucidated. These studies have been central to the progressive story of $Fe(CO)_5$, being the first to show that $[Fe(CO)_4]$ has a triplet ground state, thereby explaining why thermal substitution reactions of $Fe(CO)_5$ occur at such a slow rate. In addition, matrix isolation has brought to light the interesting non-Berry psuedorotation isomerisation of this complex. Matrix isolation studies do have their drawbacks. They give little or no kinetic information and also there is no guarantee that the structure adopted in the matrix environment is the same as that in the solution or gas phase.

Solution phase studies of the photochemistry of $Fe(CO)_5$ are few. Time-resolved spectroscopic techniques have been central to the detection of transient intermediates in solution, the solvent coordinated complex $Fe(CO)_4{\cdot}(C_6D_6)$ being observed using TRIR. It has also been shown that photosubstitution of two $Fe(CO)_5$ carbonyls is possible in solution by a single-photon process, the role of triplet intermediates being central to the mechanism devised to explain this result.

A number of the studies on $Fe(CO)_5$ have been undertaken in the gas phase. It has been possible to generate highly unsaturated intermediates such as $[Fe(CO)_2]$ and [Fe(CO)]. TRIR has proven invaluable in studying the relative product distribution, kinetics of formation and reaction chemistry of the unsaturated intermediates generated in the gas phase by photolysis of $Fe(CO)_5$ at different wavelengths. The unsaturated intermediates are formed in a stepwise manner rather than as a result of a concerted process. For example, $[Fe(CO)_3]$ is formed by loss of CO from $[Fe(CO)_4]$ and not by concerted loss of two carbonyl groups from $Fe(CO)_5$. Using supersonic beam techniques it has been possible to investigate further the energy disposal within the nascent photoproducts and gain a greater insight into the underlying photochemical processes.

Femtosecond spectroscopy has been used to investigate multiple photon absorption phenomena in $Fe(CO)_5$. The results have shown that a concerted mechanism

rules the photodissociation process; Fe(CO) being formed in 100 fs after absorption of two photons of 400 nm. By studying the reaction on the fs timescale it is possible to gain a deeper understanding if the mechanism of the process and looks at the chemistry occurring within the period of a single vibration.

The reaction chemistry of $[Fe(CO)_4]$ and $[Fe(CO)_3]$ with a number of ligands has been investigated and, in all cases, the spin states of the intermediates is central to the understanding of both the rates of reaction and the products formed. Reactions of $[Fe(CO)_4]$ with simple two-electron donors such as CO or ethene are several orders of magnitude slower than for other unsaturated first-row transition metal carbonyl fragments. This has been attributed to the spin forbidden nature of the reaction owing to the triplet ground state of $[Fe(CO)_4]$.

With the use of all these experimental techniques and others, such as excited state resonance Raman spectroscopy, the future study of the photochemistry of organometallics promises to be exciting. Of course, as these experiments probe the mechanism of reactions in greater detail, a whole set of new questions will be raised. Developments in laser chemistry will open several avenues for research, the continuation of the study into single versus multiple photon processes being but one example. Little is known about the excited states of unsaturated organometallic intermediates and there is certainly scope for much work here with the new and upcoming experimental techniques especially using the collision-free environment of a supersonic molecular beam.

This article has focused on the photochemistry of $Fe(CO)_5$ and has shown how fascinating the chemistry of the intermediates generated from such an archetypal transition-metal carbonyl can be. There is scope for in-depth investigations of other carbonyl complexes and for adaptation of the techniques discussed here for the study of more complex substituted complexes. It will be interesting to move the studies on from looking at the chemistry of unsaturated metal carbonyl fragments where reacting ligands are small to those systems where more complex processes take place. This would then lead to the possible study of the chemistry of catalytically-active carbonyl complexes. By using photochemistry it will be possible to generate key intermediates in the catalytic cycle and study their reaction chemistry with both known and new potential substrates.

In this review, reference has been made to the results from theory on a number of occasions. These results have augmented the experimental studies, allowing for a more thorough understanding of the processes intimately involved both in the photogeneration of coordinatively unsaturated intermediates and also in the reaction chemistry of these fragments. In the future, theoretical studies on molecules in the ground and first excited states will prove invaluable and, together with modelling of the dynamics of photodissociation, will assist the study of the photoprocesses in organometallics. Even if development of quantitative models for the dynamics of reactions are still some way off, qualitative approaches will serve as useful, unifying framework for future work.

We now look forward to advances in experimental technique and in the understanding of the fundamental processes intimately involved in photochemistry.

Acknowledgements

Girton College, Cambridge is thanked for a Research Fellowship. The referee is thanked for raising important points.

References

[1] M. Poliakoff, E. Wietz, Acc. Chem. Res. 20 (1987) 408.
[2] M. Poliakoff, J.J. Turner, J. Chem. Soc. Faraday Trans. 2 (70) (1974) 93.
[3] S.K. Nayak, T.J. Burkey, Inorg. Chem. 31 (1992) 1127.
[4] J.T. Yardley, B. Gitlin, G. Nathanson, A.M. Rosan, J. Chem. Phys. 74 (1981) 370.
[5] R.J. Ryther, E. Weitz, J. Phys. Chem. 95 (1991) 9841.
[6] R.J. Ryther, E. Weitz, J. Phys. Chem. 96 (1992) 2560.
[7] (a) D. Braga, F. Grepioni, A.G. Orpen, Organometallics 12 (1993) 1481. (b) J. Huang, K. Hedberg, R.K. Pomeroy, Organometallics 7 (1988) 2049.
[8] A.R. Rossi, R. Hoffmann, Inorg. Chem. 14 (1975) 365.
[9] R. Hoffmann, J.M. Howell, E.L. Muetterties, J. Am. Chem. Soc. 94 (1972) 3047.
[10] A.W. Ehlers, G. Frenking, Organometallics 14 (1995) 423.
[11] T Zeigler, V. Tschinke, C. Ursenbach, J. Am. Chem. Soc. 109 (1987) 4825.
[12] T. Zeigler, G.J. Snijders, E.J. Baerends, J. Chem. Phys. 24 (1981) 1271.
[13] (a) D.F. Keely, R.E. Johnson, J. Inorg. Nucl. Chem. 11 (1959) 33. (b) E.E. Seifert, R.J. Angelici, J. Organomet. Chem. 8 (1967) 374. (c) W. Reppe, W. Schweckendiek, J. Leibigs Ann. Chem. 560 (1948) 104. (d) R.B. Jordan, Reaction Mechanisms of Inorganic and Organometallic Systems, Oxford University Press, Oxford, 1991.
[14] (a) R. Huq, A.J. Poë, S. Chawla, Inorg. Chim. Acta 38 (1980) 121. (b) M.A. Cobb, B. Hungate, A.J. Poë, J. Chem. Soc. Dalton Trans. (1976) 2226. (c) J.J. Levison, S.D. Robinson, J. Chem. Soc. A (1970) 639. (d) R. Colton, R.H. Farthing, Aust. J. Chem. 20 (1967) 1283.
[15] M. Poliakoff, J.J. Turner, J. Chem. Soc. Dalton Trans. (1974) 2276
[16] M. Poliakoff, Chem. Soc. Rev. (1978) 527
[17] For an introduction to matrix photochemistry see: (a) M.J. Almond, Short-lived Molecules, Ellis Horwood, London, 1990. (b) M.J. Almond, A.J. Downs, in: R.J.H. Clark, R.E. Hester (Eds.), Advances in Spectroscopy, vol. 17, Wiley, New York, 1989.
[18] M. Poliakoff, J.J. Turner, J. Chem. Soc. Dalton Trans. (1973) 1351.
[19] J.H. Darling, J.S. Ogden, J. Chem. Soc. Dalton Trans. (1972) 2496.
[20] E. Kochanski (Ed.), Photoprocesses in Transition Metal Complexes, Klewer Academic, Dordrecht, 1992.
[21] J.A. Timney, in: R.B. King (Ed.), Encyclopedia of Inorganic Chemistry, vol. 8, Wiley, Chichester, 1994.
[22] J.K. Burdett, M. Poliakoff, J.A. Timney, J.J. Turner, Inorg. Chem. 17 (1978) 948.
[23] J.K. Burdett, H. Dubost, M. Poliakoff, J.J Turner, in: R.J.H. Clark, R. Hester (Eds.), Advances in Infrared and Raman Spectroscopy, Heyden, London, 1976.
[24] B. Davies, A. McNeish, M. Poliakoff, J.J. Turner, J. Am. Chem. Soc. 99 (1977) 7573.
[25] L.M. Haines, M.B.H. Stiddard, Adv. Inorg. Radiochem. 12 (1969) 53.
[26] J.K. Burdett, J. Chem. Soc. Faraday Trans. 2 (70) (1974) 93.
[27] I.N. Douglas, R. Grinter, A.J. Thompson, Mol. Phys. 28 (1974) 1377.
[28] T.J. Barton, R. Grinter, A.J. Thompson, B. Davies, M. Poliakoff, J. Chem. Soc. Chem. Commun. (1977) 841.
[29] M. Poliakoff, J. Chem. Soc. Dalton Trans. (1974) 210
[30] M.A. Graham, R.N. Perutz, M. Poliakoff, J.J. Turner, J. Organomet. Chem. 34 (1972) C34.
[31] S.C. Fletcher, M. Poliakoff, J.J. Turner, Inorg. Chem. 25 (1986) 3597.
[32] C.H.F. Peden, S.F. Parker, P.H. Barrett, R.G. Pearson, J. Phys. Chem. 87 (1983) 2329.

[33] J.K. Burdett, Coord. Chem. Rev. 27 (1978) 1.
[34] R.L. Sweaney, J. Am. Chem. Soc. 103 (1981) 2410.
[35] T.A. Seder, S.P. Church, A.J. Ouderkirk, E. Weitz, J. Am. Chem. Soc. 107 (1985) 1432.
[36] J.A. Timney, Inorg. Chem. 18 (1979) 2502.
[37] D. Guenzburger, E.M. Baggio-Saitovitch, M.A. De Paoli, S.M. de Oliveira, J. Chem. Phys. 80 (1984) 730.
[38] G.M. Bancroft, R.H. Platt, Adv. Inorg. Radiochem. 6 (1964) 433.
[39] V.I. Goldanskii, R.H. Herber (Eds.), Chemical Applications of Mössbauer Spectroscopy, Academic Press, New York, 1968.
[40] (a) D.F. McIntosh, R.P. Messmer, G.A. Ozin, Inorg. Chem. 20 (1981) 3640. (b) F.J. Litterst, H. Micklitz, Phys. Rev. Lett. 33 (1974) 480. (c) P.H. Barrett, H. Micklitz, Phys. Rev. Lett. 28 (1972) 1547.
[41] P.H. Barrett, M. Pasternak, J. Chem. Phys. 71 (1979) 3837.
[42] S. Parker, C.H.F. Peden, P.H. Barrett, R.G. Pearson, Inorg. Chem. 22 (1984) 2813.
[43] W.A. Goddard, G.A. Ozin, W.J. Power, T.H. Upton, 100 (1978) 4750.
[44] S.P Church, F.-W. Grevels, H. Hermann, K. Schaffner, Inorg. Chem. 23 (1984) 3830.
[45] S.P. Church, F.-W. Grevels, H. Hermann, K. Schaffner, Inorg. Chem. 24 (1985) 418.
[46] S.P. Church, F.-W. Grevels, H. Hermann, J.M. Kelly, W.E. Klotzbücher, K. Shaffner, J. Chem. Soc. Chem. Commun. (1985) 594.
[47] S.K. Nayak, T.J. Burkey, Inorg. Chem. 33 (1994) 2236.
[48] T.A. Seder, A.J. Ouderkirk, E. Weitz, J. Phys. Chem. 85 (1986) 1977.
[49] D.M. Rayner, Y. Ishikawa, C.E. Brown, P.A. Hackett, J. Chem. Phys. 94 (1991) 5471.
[50] G. Cardaci, Inorg. Chem. 13 (1974) 2974.
[51] E. Weitz, J.R. Wells, R.J. Ryther, P. House, in: J. Chaiken (Ed.), Laser Chemistry of Organometallics ACS Symposium Series 530, American Chemical Society, Washington, DC, 1993.
[52] (a) S. Yu, X. Xu, R. Lingle, J.B. Hopkins, J. Am. Chem. Soc. 112 (1990) 3668. (b) L. Wang, X. Zhu, K.G. Spears, J. Am. Chem. Soc. 110 (1988) 8695.
[53] E. Weitz, J. Phys. Chem. 91 (1987) 3945.
[54] C.E. Housecroft, K. Wade, B.C. Smith, J. Organomet. Chem. 170 (1979) C1.
[55] J.J. Turner, J.K. Burdett, R.N. Perutz, M. Poliakoff, Pure Appl. Chem. 49 (1977) 271.
[56] G.H. Atkinson, Time-Resolved Vibrational Spectroscopy, Academic Press, New York, 1983.
[57] C.A. Udovich, R.J. Clark, H. Haas, Inorg. Chem. 8 (1969) 1066.
[58] R.J. Clark, Inorg. Chem. 3 (1964) 1395.
[59] G. Nathanson, B. Gitlin, A.M. Rosan, J.T. Yardley, J. Chem. Phys. 74 (1981) 361.
[60] J.T. Yardley, Introduction to Molecular Energy Transfer, Academic Press, New York, 1980.
[61] (a) F. Adams, R. Gijbels, R. van Grieken (Eds.), Inorganic Mass Spectrometry, Wiley, New York, 1988. (b) C.E. Klots, J. Phys. Chem. 75 (1971) 1526.
[62] J.W.T. Spinks, R.J. Woods, An Introduction to Radiation Chemistry, Wiley, New York, 1990.
[63] (a) T.R. Fletcher, R.N. Rosenfeld, J. Am. Chem. Soc. 105 (1983) 6358. (b) T.A. Seder, S.P. Church, E. Weitz, J. Am. Chem. Soc. 108 (1986) 4721.
[64] D. Hayes, E. Weitz, J. Phys. Chem. 95 (1991) 2723.
[65] J.K. Burdett, Molecular Shapes, Wiley, New York, 1980.
[66] S.J. Gravelle, E. Weitz, J. Am. Chem. Soc. 112 (1990) 7839.
[67] (a) T. Majima, T. Ishii, Y. Matsumoto, M. Takami, J. Am. Chem. Soc. 111 (1989) 2417. (b) T. Majima, Coord. Chem. Rev. 132 (1994) 141.
[68] A.E. Siegman, Lasers, Oxford University Press, Oxford, 1986.
[69] R.D. Levine, R.B. Bernstein, Molecular Reaction Dynamics and Chemical Reactivity, Oxford University Press, New York, 1987.
[70] K.J. Laidler, Chemical Kinetics, Harper and Row, New York, 1987.
[71] For photofragment spectroscopy of metal carbonyls see: (a) D.J. Bamford, S.V. Filseth, M.F. Folz, J.W. Hepburn, C.B. Moore. J. Chem. Phys. 82 (1985) 3032. (b) N. Sivakumar, I Burak, P.L. Houston, in: W.C. Stwalley, M. Lapp (Eds.), Advances in Laser Science, American Institute of Physics, New York, 1985.
[72] I.M. Waller, H.F. Davis, J.W. Hepburn, J. Phys. Chem. 91 (1987) 506.

[73] U. Ray, S.L. Brandow, G. Bandukwalla, B.K. Venkataraman, Z. Zhang, M. Vernon, J. Chem. Phys. 89 (1988) 4092.
[74] I.M. Waller, J.W. Hepburn, J. Chem. Phys. 88 (1988) 6658.
[75] N. Sivakumar, I. Burak, W.-Y. Cheung, P.L. Houston, J.P. Hepburn, J. Phys. Chem. 89 (1985) 3609.
[76] D. Guenzburger, E.M. Baggio-Saitovitch, M.A. De Paoli, H. Manela, J. Chem. Phys. 80 (1984) 735.
[77] (a) F.J. Schlenker, F. Bouchard, I.M. Waller, J.W. Hepburn, J. Chem. Phys. 93 (1990) 7110. (b) N. Rösch, M. Kotzian, H. Jörg, H. Schröder, B. Rager, S. Metev, J. Am. Chem. Soc. 108 (1986) 4238.
[78] (a) D.M. Rayner, Y. Ishikawa, C.E. Brown, P.A. Hackett, J. Phys. Chem. 94 (1990) 2404. (b) J.A. Ganske, R.N. Rosenfeld, J. Phys. Chem. 93 (1989) 1959. (c) D.M. Rayner, Y. Ishikawa, P.A. Hackett, J. Phys. Chem. 92 (1988) 3863.
[79] L. Banares, T. Baumert, M. Bergt, B. Keifer, G. Gerber, Chem. Phys. Lett. 267 (1997) 141.
[80] A.H. Zewail, Science 242 (1988) 1645.
[81] A. Zewail, Faraday Discuss. Chem. 91 (1991) 207.
[82] R.L. Jackson, Acc. Chem. Res. 25 (1992) 581.
[83] N. Bloembergen, C.D. Cantrell, D.M. Larsen, in: A. Mooradian, T. Jaeger, P. Stokseth (Eds.), Tunable Lasers and Applications, Springer-Verlag, New York, 1976.
[84] M. Poliakoff, Spectrochim. Acta A 43 (1987) 217.
[85] M. Poliakoff, J.J Turner, in: C.B. Moore (Ed.), Chemical and Biological Applications of Lasers, Academic Press, New York, 1981.
[86] A.I. Cooper, M. Poliakoff, Chem. Phys. Lett. 212 (1993) 611.
[87] M. Hidai, Y. Mizobe, Chem. Rev. 95 (1995) 1115.
[88] E.W. Abel, I.S. Butler, C.R. Jenkins, J. Organomet. Chem. 8 (1967) 382.
[89] (a) T.A. Albright, J.K. Burdett, M.-H. Whangbo, Orbital Interactions in Chemistry, Wiley, New York, 1985. (b) A.R. Rossi, R. Hoffmann, Inorg. Chem. 14 (1975) 365.
[90] S.A. Goldfield, K.N Raymond, Inorg. Chem. 13 (1974) 770.
[91] A.F. Schreiner, T.L. Brown, J. Am. Chem. Soc. 90 (1968) 3366.
[92] F.A. Cotton, T. LaCour, A.G. Stanislowski, J. Am. Chem. Soc. 96 (1974) 754.
[93] S.W. Kirtley, M.A. Andrews, R. Bau, G.G. Grynkewich, T.J. Marks, D.L. Tipton, B.R. Whitlesey, J. Am. Chem. Soc. 99 (1977) 7154.
[94] R.N. Perutz, J.J. Turner, Inorg. Chem. 14 (1975) 262.
[95] (a) J.K. Burdett, M.A. Graham, R.N. Perutz, M. Poliakoff, A.J. Rest, J.J Turner, R.F. Turner, J. Am. Chem. Soc. 97 (1975) 4805. (b) M.A. Graham, A.J. Rest, J.J. Turner, J. Organomet. Chem. 24 (1970) C54.
[96] J.D. Black, P.S. Braterman, J. Am. Chem. Soc. 97 (1975) 2908.
[97] (a) J.M. Kelly, D.V. Bent, H. Hermann, D. Schulte-Fröhlinde, E. Koerner von Gustorf, J. Organomet. Chem. 24 (1970) C54. (b) J.M. Kelly, H. Hermann, E. Koerner von Gustorf, J. Chem. Soc. Chem. Commun. (1973) 105. (c) J.A. McIntire, J. Phys. Chem. 74 (1970) 2403.
[98] M. Poliakoff, A. Ceulemans, J. Am. Chem. Soc. 106 (1984) 50.
[99] D.G. Rouvray, Chem. Soc. Rev. 3 (1974) 355.
[100] A. Ceulemans, D. Beyens, L.G. Vanquickenborne, J. Am. Chem. Soc. 104 (1984) 5824.
[101] M. Elian, R. Hoffmann, Inorg. Chem. 14 (1975) 1058.
[102] E.W. Abel, F.G.A. Stone, G. Wilkinson (Eds.), Comprehensive Organometallic Chemistry, vol. 4, Pergamon Press, Oxford, 1982.
[103] H. Flekner, F.-W. Grevels, D.J. Hess, J. Am. Chem. Soc. 106 (1984) 2027.
[104] H. Angermund, A.K. Bandlyopadhyay, F.-W. Grevels, F. Mark, J. Am. Chem. Soc. 111 (1989) 4656.
[105] S.J. Gravelle, L.J. van de Burgt, E. Weitz, J. Phys. Chem. 97 (1993) 5272.
[106] R.H. Crabtree, The Organometallic Chemistry of the Transition Metals, Wiley, New York, 1994.
[107] (a) E.R. Grant, M.E. Miller, B.H. Weiller, J. Am. Chem. Soc. 107 (1987) 352. (b) E.R. Grant, B.H. Weiller, J. Am. Chem. Soc. 107 (1987) 1051.
[108] W. Wang, A.A. Narducci, P.G. House, E. Weitz, J. Am. Chem. Soc. 118 (1996) 8654.

[109] C. Daniel, J. Phys. Chem. 95 (1991) 2394.
[110] J.R. Wells, P.G. House, E. Weitz, J. Phys. Chem. 98 (1994) 3343.
[111] (a) R.H. Crabtree, Angew. Chem. Int. Ed. Engl. 32 (1993) 789. (b) R.H. Crabtree, Acc. Chem. Res. 23 (1990) 95.
[112] G.E. Gadd, R.K. Upmacis, M. Poliakoff, J.J. Turner, J. Am. Chem. Soc. 108 (1986) 2547.
[113] D.M. Hayes, E. Weitz, J. Phys. Chem. 95 (1991) 2723.
[114] P.G. House, E. Weitz, Chem. Phys. Lett. 266 (1997) 239.